arXiv:hep-th/9803238v2 3 Dec 1998

Weak Field Expansion of Gravity : Graphs, Matrices and Topology *

Shoichi ICHINOSE[a] †and Noriaki IKEDA[b] ‡
[a] Department of Physics, University of Shizuoka,
Yada 52-1, Shizuoka 422-8526, Japan
[b] Research Institute for Mathematical Sciences,
Kyoto University, Kyoto 606-01, Japan

March, 1998

Abstract

We present some approaches to the perturbative analysis of the classical and quantum gravity. First we introduce a graphical representation for a global SO(n) tensor $(\partial)^d h_{\alpha\beta}$, which generally appears in the weak field expansion around the flat space: $g_{\mu\nu} = \delta_{\mu\nu} + h_{\mu\nu}$. Making use of this representation, we explain 1) Generating function of graphs (Feynman diagram approach), 2) Adjacency matrix (Matrix approach), 3) Graphical classification in terms of "topology indices" (Topology approach), 4) The Young tableau (Symmetric group approach). We systematically construct the global SO(n) invariants. How to show the independence and completeness of those invariants is the main theme. We explain it taking simple examples of $\partial\partial h-$, and $(\partial\partial h)^2-$ invariants in the text. The results are applied to the analysis of the independence of general invariants and (the leading order of) the Weyl anomalies of scalar-gravity theories in "diverse" dimensions (2,4,6,8,10 dimensions).

- Key Words: weak field expansion, gravity, graphical representation, matrix representation, topology, SO(n)-invariants.
- PACS No.: 02.70.-c, 02.40.-k, 04.50.+h, 04.62.+v, 11.25.Db.

*hep-th/9803238 , US-98-03
†E-mail address: ichinose@u-shizuoka-ken.ac.jp
‡E-mail address: nori@kurims.kyoto-u.ac.jp

1 Introduction

Stimulated by the string theory, the higher (than 4) dimensional (super) gravity becomes more and more important as its low-energy (field theory) limit. In order to understand the coming new concept involved in the string dynamics, it seems to become important to analyze the higher dim gravity as the quantum field theory. Generally, however, the higher dim gravity is technically difficult to treat with. We must deal with higher dim general invariants. (For example, the conformal anomaly terms in n dim are of the type: (Riemann tensor)$^{n/2}$.) The present analysis aims at developing some useful approaches in such analysis.

In n-dimensional Euclidean (Minkowski) flat space(-time), fields are classified as scalar, spinor, vector, tensor ... , by the transformation property under the global SO(n) (SO(n-1,1)) transformation of space(-time) coordinates.

$$x^{\mu\prime} = M^{\mu}_{\ \nu} x^{\nu} \quad , \quad M \in SO(n) \quad , \tag{1}$$

where M is a $n \times n$ matrix of SO(n)(SO(n-1,1)) [1]. As for the lower spin fields, the field theory is well defined classically and quantumly.

The general curved space is described by the general relativity which is based on invariance under the general coordinate transformation. Its infinitesimal form is written as

$$x^{\mu\prime} = x^{\mu} - \epsilon^{\mu}(x) \quad , \quad |\epsilon| \ll 1 \quad ,$$
$$\delta g_{\mu\nu} = g_{\mu\lambda}\nabla_{\nu}\epsilon^{\lambda} + g_{\nu\lambda}\nabla_{\mu}\epsilon^{\lambda} + O(\epsilon^2) = \epsilon^{\lambda}\partial_{\lambda}g_{\mu\nu} + g_{\mu\lambda}\partial_{\nu}\epsilon^{\lambda} + g_{\nu\lambda}\partial_{\mu}\epsilon^{\lambda} + O(\epsilon^2) \quad , \tag{2}$$

where ϵ^{μ} is an infinitesimal local free parameter. The general invariant which is composed of purely geometrical quantities and whose mass dimension [2] is $(Mass)^2$, is uniquely given by Riemann scalar curvature R defined by

$$\Gamma^{\lambda}_{\mu\nu} = \frac{1}{2}g^{\lambda\sigma}(\partial_{\mu}g_{\sigma\nu} + \partial_{\nu}g_{\sigma\mu} - \partial_{\sigma}g_{\mu\nu}) \quad , R^{\lambda}_{\ \mu\nu\sigma} = \partial_{\nu}\Gamma^{\lambda}_{\mu\sigma} + \Gamma^{\lambda}_{\tau\nu}\Gamma^{\tau}_{\mu\sigma} - \nu \leftrightarrow \sigma \quad ,$$
$$R_{\mu\nu} = R^{\lambda}_{\ \mu\nu\lambda} \quad , \quad R = g^{\mu\nu}R_{\mu\nu} \quad , \quad g = \det g_{\mu\nu} \quad . \tag{3}$$

It is well-known that the general relativity can be constructed purely within the flat space first by introducing a symmetric second rank tensor (Fierz-Pauli field) and then by requiring consistency in the field equation in a perturbative way of the weak field [1]. In the present case, we can obtain the perturbed lagrangian simply by the perturbation around the flat space.

$$g_{\mu\nu} = \delta_{\mu\nu} + h_{\mu\nu} \quad , \quad |h_{\mu\nu}| \ll 1 \quad . \tag{4}$$

Then the transformation (2) is expressed as

$$\delta h_{\mu\nu} = \partial_{\mu}\epsilon^{\nu} + h_{\mu\lambda}\partial_{\nu}\epsilon^{\lambda} + \frac{1}{2}\epsilon^{\lambda}\partial_{\lambda}h_{\mu\nu} + \mu \leftrightarrow \nu + O(\epsilon^2) \quad . \tag{5}$$

[1] Hereafter we take the Euclidean case for simplicity.

[2] We take the natural units: $c = \hbar = 1$.

In the right-hand side (RHS), there appear h^0-order terms and h^1-order terms. Therefore the general coordinate transformation (5) does *not* preserve the weak-field ($h_{\mu\nu}$) perturbation order. (This is the reason why the result based on the lower-order weak-field perturbation restores all higher-order terms after the requirement of the general invariance.) Riemann scalar curvature is also expanded as

$$\begin{aligned} R = \partial^2 h - \partial_\mu \partial_\nu h_{\mu\nu} - h_{\mu\nu}(\partial^2 h_{\mu\nu} - 2\partial_\lambda \partial_\mu h_{\nu\lambda} + \partial_\mu \partial_\nu h) \\ +\tfrac{1}{2}\partial_\mu h_{\nu\lambda} \cdot \partial_\nu h_{\mu\lambda} - \tfrac{3}{4}\partial_\mu h_{\nu\lambda} \cdot \partial_\mu h_{\nu\lambda} + \partial_\mu h_{\mu\lambda} \cdot \partial_\nu h_{\nu\lambda} \\ -\partial_\mu h_{\mu\nu} \cdot \partial_\nu h + \tfrac{1}{4}\partial_\mu h \cdot \partial_\mu h + O(h^3) \quad , \end{aligned} \tag{6}$$

where $h \equiv h_{\mu\mu}$. RHS is expanded to the infinite power of $h_{\mu\nu}$ due to the presence of the 'inverse' field of $g_{\mu\nu}$, $g^{\mu\nu}$, in (3).

It is explicitly checked that R, defined perturbatively by the RHS of (6), transforms, under (5), as a scalar $\delta R(x) = \epsilon^\lambda(x)\partial_\lambda R(x)$, at the order of $O(h)$. Because the general coordinate symmetry does not preserve the the weak-field ($h_{\mu\nu}$) perturbation order, we need $O(h^2)$ terms in (6) in order to verify $\delta R(x) = \epsilon^\lambda(x)\partial_\lambda R(x)$, at the order of $O(h)$. The first two terms of RHS of (6), $\partial^2 h$ and $\partial_\mu \partial_\nu h_{\mu\nu}$, are two independent global SO(n) invariants at the order O(h). We may regard the weak field perturbation using (4) as a sort of 'linear' representation of the general coordinate symmetry, where all general invariant quantities are generally expressed by the infinite series of power of $h_{\mu\nu}$, and there appears no 'inverse' fields. One advantage of the linear representation is that the independence of invariants, as a local function of x^μ, can be clearly shown because all quantities are written only by $h_{\mu\nu}$ and its derivatives. We analyze some basic aspects of the weak-field expansion and develop a useful graphical technique.

It is a classical theme to obtain invariants with respect to a group[2]. One established method to obtain $SO(n)$-invariants is to use the representation theory of the symmetric group, or the Young tableaus [3][4]. It is reviewed in App.A, for the comparison with the present work. We propose some new methods in this paper. The basic idea is to express every $SO(n)$-invariant graphically (Sec.2) and treat every procedure (suffix contraction in the tensor product, classification of invariants, enumeration, e.t.c.) in relation to graphs. A part of these new methods is already used in Ref.[5] where $\partial\partial h$-tensor is mainly considered. Their usefulness is confirmed by the complete classification of $(\partial\partial h)^3$-invariants. The present paper treats a more general case: h, ∂h, $\partial\partial h$, $\partial\partial\partial h$, $\cdots$.

In Sec.2 the graphical representation of tensors and invariants is introduced. We start with the field theory approach to the present problem in Sec.3. It is familiar in the perturbative field theory to use the Feynman diagrams to express all expanded terms. The generating functional which generates every $SO(n)$-invariant is given. There exist, in the graph theory[6], some matrix-representations to express a graph. We take the *adjacency matrix* and apply it to the present problem in Sec.4. All graphs of invariants is systematically listed using the graph topology in Sec.5. In Sec.6, the completeness of the graph enumeration is shown from the viewpoint of the suffix-permutation symmetry. In order to identify every graph succinctly, we introduce a set of *indices* in Sec.7. It is explicitly shown that every $(\partial\partial h)^2$-invariant

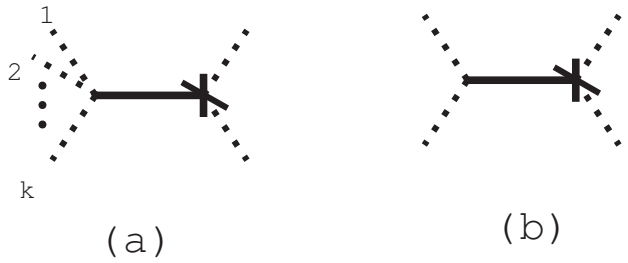

Fig.1 (a) (k+2)-tensor (9); (b) 4-tensor $\partial_\mu \partial_\nu h_{\alpha\beta}$

is identified by five indices. In Sec.8, we explain how to read these indices from the adjacency matrices. We apply the present results to some gravitational problem in Sec.9. Finally we conclude in Sec.10. Four appendices are prepared to complement the text. In App.A, we review the Young tableau approach in relation to the present problem. Some examples of adjacency matrices are given in App.B. In App.C we explain some indices in detail. The gauge-fixing condition and the corresponding graphical rule are explained in App.D.

2 Graphical Representation of $\partial^d h$-tensors and invariants

We treat a general invariant made from any contraction of the following quantity:

$$(\partial_{\mu_1}\partial_{\mu_2}\cdots\partial_{\mu_{d_1}}h_{\lambda_1\rho_1})(\partial_{\nu_1}\partial_{\nu_2}\cdots\partial_{\nu_{d_2}}h_{\lambda_2\rho_2})\cdots(\partial_{\tau_1}\partial_{\tau_2}\cdots\partial_{\tau_{d_B}}h_{\lambda_B\rho_B})\ . \tag{7}$$

We define two basic indices of the invariant: the mass dimension(= No. of differentials), D, and the number of $h_{\lambda\rho}$(=No. of "bonds" defined below), B. If D and B are given, we can define another index, the *partition* of D, $(d_1, d_2, d_3, \cdots, d_B)$, corresponding to a division of differentiations. The partition satisfies the following relation.

$$D = \sum_{k=1}^{B} d_k \quad , \quad d_k : \ 0, 1, 2, 3, \cdots \quad , \tag{8}$$

where d_k is the number of differentiations of $h_{\lambda_k\rho_k}$.

We graphically represent a global $SO(n)$ tensor,

$$\partial_{\mu_1}\partial_{\mu_2}\cdots\partial_{\mu_k}h_{\lambda\rho} \quad . \tag{9}$$

as in Fig.1[5]. The graph respects all suffix-permutation symmetries of $\partial_{\mu_1}\partial_{\mu_2}\cdots\partial_{\mu_k}h_{\lambda\rho}$:

1. totally symmetric with repect to $(\mu_1, \mu_2, \cdots, \mu_k)$,
2. symmetric with repect to λ and ρ.

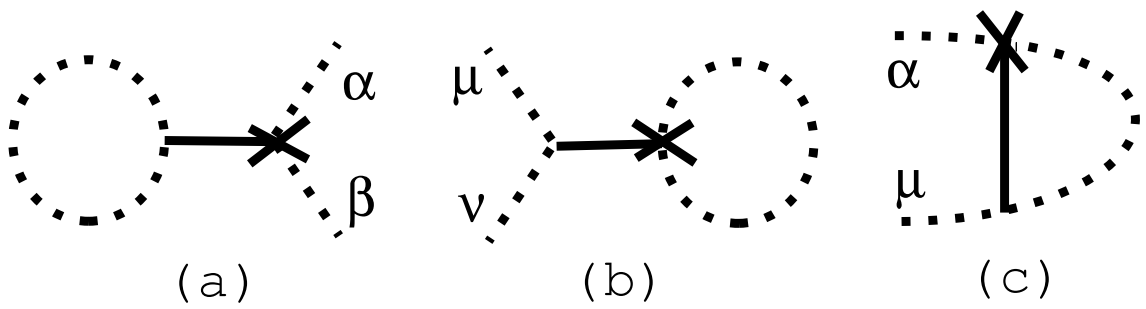

Fig.2 2-tensors of $\partial^2 h_{\alpha\beta}$, $\partial_\mu \partial_\nu h_{\alpha\alpha}$ and $\partial_\mu \partial_\beta h_{\alpha\beta}$

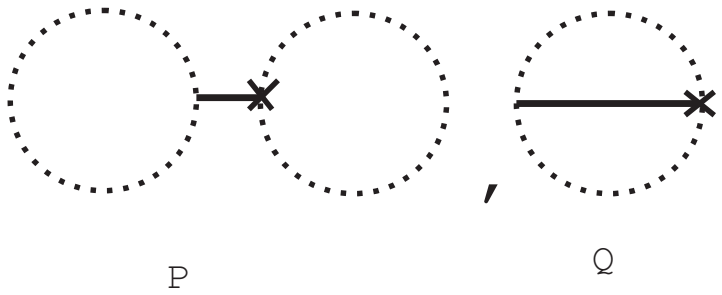

Fig.3 Invariants of $P \equiv \partial_\mu \partial_\mu h_{\alpha\alpha}$ and $Q \equiv \partial_\alpha \partial_\beta h_{\alpha\beta}$.

Let us introduce some definitions.

Def 1 [5] We call dotted lines *suffix-lines*, a rigid line a *bond*, a vertex with a crossing mark a *h-vertex* and that without it a *der-vertex*. We also specifically call the last one *d^k-vertex* where k is the number of suffix-lines which the crossing-mark-less vertex has. We often use *dd-vertex* instead of *d^2-vertex*.

Def 2 [5] The suffix *contraction* is graphically expressed by connecting the two corresponding suffix-lines.

For example, 2nd rank tensors (2-tensors) [3] : $\partial^2 h_{\alpha\beta}$, $\partial_\mu \partial_\nu h_{\alpha\alpha}$, $\partial_\mu \partial_\beta h_{\alpha\beta}$, which are made from the Fig.1b by connecting two suffix-lines, are expressed as in Fig.2. Two independent invariants (0-tensors) : $P \equiv \partial_\mu \partial_\mu h_{\alpha\alpha}$, $Q \equiv \partial_\alpha \partial_\beta h_{\alpha\beta}$, which are made from Fig.2 by connecting the remaining two suffix-lines, are expressed as in Fig.3. P and Q are all possible invariants of $\partial\partial h$-type. All suffix-lines of Fig.3 are closed. We easily see the following lemma is valid.

Lemma 1 [5] Generally all suffix-lines of invariants are *closed*. We call a closed suffix-line a *suffix-loop*.

If we neglect degeneracies due to symmetries among suffixes. the number of

[3] We call k-th rank tensor *k-tensor* hereafter.

different contractions of the general tensor (7) to make invariants is given as

$$(N-1)(N-3)\cdots 3\cdot 1 = \frac{(N)!}{2^{\frac{N}{2}}(\frac{N}{2})!} \quad , \quad N \equiv D+2B \quad , \tag{10}$$

This relation turns out to be important to show the enumeration of all graphs with no missing graphs.

3 Generating Functional for Graphs: Feynman Diagram Approach

We can construct the generating functional for all possible graphs. It is an application of the field theoretic approach to our graphical representations. Let us consider the following Lagrangian in 2 space-dimension [4] .

$$\mathcal{L}[\phi,\omega_1,\omega_2] = \mathcal{L}_0 + \mathcal{L}_I \quad ,$$
$$\mathcal{L}_0 = \frac{1}{2}\phi^2 + \omega_1\omega_2 \quad , \quad \mathcal{L}_I[\phi,\omega_1,\omega_2] = \omega_1 \sum_{i=0}^{\infty} g_i\phi^i + \lambda\phi^2\omega_2 \quad . \tag{11}$$

The dotted lines in Sec.2 are represented by $\phi\phi$ propagators and the rigid lines by $\omega_1\omega_2$ propagators. λ-interaction term describes the h-vertex and g_i-interaction term describes the d^i-vertex See Fig.4. We assign mass-dimension as follows.

$$[\mathcal{L}] = M^2 \quad , \quad [\phi] = M \quad , \quad [\omega_1] = M^2 \quad , \quad [\omega_2] = M^0 \quad . \tag{12}$$

Then we obtain

$$[g_i] = M^{-i} \quad , \quad [\lambda] = M^0 \quad . \tag{13}$$

The generating functional of all graphs ($SO(n)$-invariants, $SO(n)$-tensors) is given by

$$\begin{aligned} W[J,K_1,K_2] &= \mathrm{e}^{\Gamma[J,K_1,K_2]} \\ &= \int \mathcal{D}\phi\mathcal{D}\omega_1\mathcal{D}\omega_2 \exp\left[\int d^2x(\mathcal{L}[\phi,\omega_1,\omega_2] + J\phi + K_1\omega_1 + K_2\omega_2)\right] \\ &= \sum_{r=0}^{\infty}\frac{1}{r!}\left[\int d^2x\mathcal{L}_I(\tfrac{\delta}{\delta J(x)},\tfrac{\delta}{\delta K_1(x)},\tfrac{\delta}{\delta K_2(x)})\right]^r \exp\int d^2x(-\tfrac{1}{2}J(x)J(x) - K_1(x)K_2(x)) \ . \end{aligned} \tag{14}$$

All graphs of connected k-tensors appear in the k-point Green function.

$$\frac{1}{k!}\frac{\delta}{\delta J(x_1)}\frac{\delta}{\delta J(x_2)}\cdots\frac{\delta}{\delta J(x_k)}\Gamma[J,K_1,K_2]\Big|_{J=0,K_1=0,K_2=0} \quad . \tag{15}$$

[4] The space-dimension is taken to be 2 in order to obtain the mass-dimensions of the couplings, (13), without introducing any additional mass parameters. Note that the present purpose is the graph classification. There the important thing is the topological structure of graphs. The space-dimension of the field theory is irrelevant.

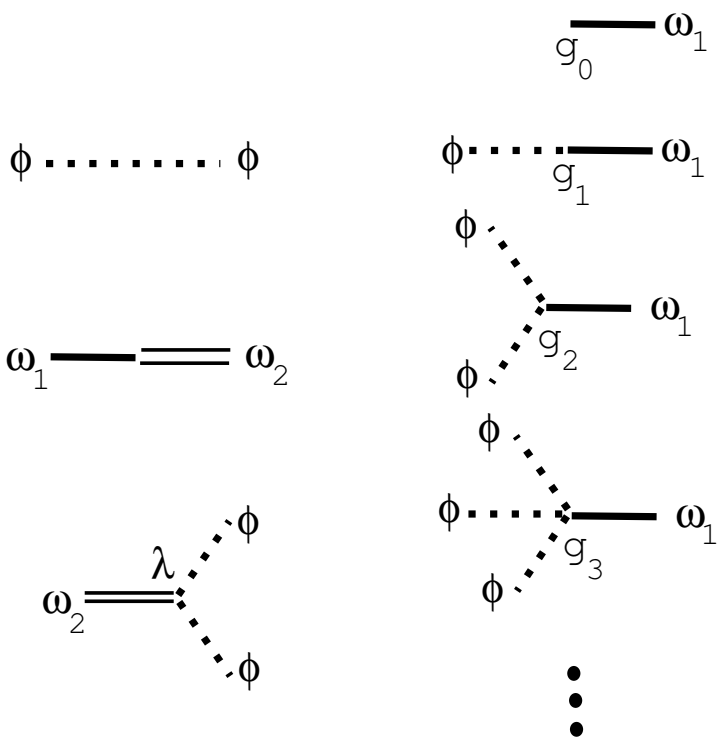

Fig.4 Feynman rule of the Lagrangian (11).

In particular all $SO(n)$-invariants appear in the $k = 0$ case above.

$$\Gamma[J, K_1, K_2]|_{J=0,K_1=0,K_2=0} \quad . \tag{16}$$

They are given by perturbation with respect to (w.r.t) the couplings $(g_0.g_1, g_2, \cdots; \lambda)$ in $\mathcal{L}_I$. For example, $(\partial\partial h)^s$-invariants $(s = 1, 2, \cdots)$ are given by $(g_2\lambda)^s$-terms $(r = 2s)$ in (16). From the coupling-dependence, we can read the mass-dimension of each graph. They show the inverse mass-dimensions of corresponding graphs. For example, from the relations $[(g_2\lambda)^s] = M^{-2s}$, $[g_4 \cdot g_2 \cdot \lambda^2] = M^{-6}$ and $[g_3 \cdot g_3 \cdot \lambda^2] = M^{-6}$ we see $(\partial\partial h)^s, \partial^4 h \cdot \partial^2 h$ and $\partial^3 h \cdot \partial^3 h$-invariants have the dimensions of M^{2s}, M^6, M^6 respectively. The coefficient in front of each expanded term are related with the *weight* of the corresponding graph which will be soon defined.

We summarize this section. We can obtain all possible graphs by enumerating all Feynman diagrams of the lagrangian (11). The vacuum polarization graphs, in which there is no external line, correspond to $SO(n)$-invariants. The diagrams in which all external lines are dotted lines, $\phi\phi$ propagators, are $SO(n)$-tensors. There is no corresponding tensorial objects for the diagrams in which external lines include rigid lines, $\omega_1\omega_2$ propagators. It is the advantage of this approach that the all invariants can be generated from the compact formulae (14) and (16).

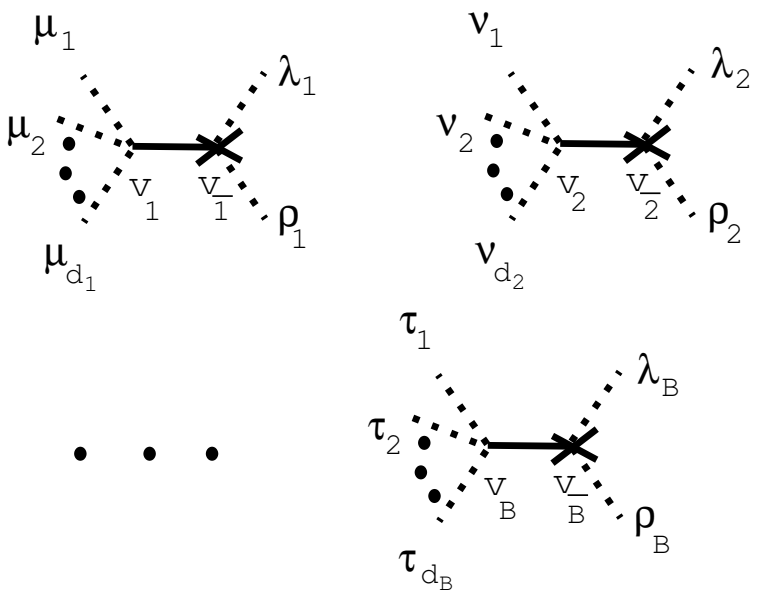

Fig.5 Graph of (7).

4 Adjacency Matrix

In Sec.2, we have defined the graphical representation of an invariant. It is well known in the graph theory[6] that a graph can be represented by a matrix defined as follows. The speciality of the present case is the "binary" structure [5] of the tensor (9) and its graph (Fig.1a).

Def 3 We name the vertices of the graph of (7) $v_1, v_{\bar{1}}; v_2, v_{\bar{2}}; \cdots; v_B, v_{\bar{B}}$ as shown in Fig.5. Then we define the *adjacency matrix* $A = [a_{IJ}]$; $I, J = 1, \bar{1}, 2, \bar{2}, \cdots, B, \bar{B}$ as follows.

i) $I \neq J$

If v_I is connected with v_J by k dotted lines (see Fig.6),

$$a_{IJ} = a_{JI} = k. \tag{17}$$

ii) $I = J$

If v_I is connected with itself by l dotted lines (see Fig.7)

$$a_{II} = 2l. \tag{18}$$

Then we see the adjacency matrix A satisfies the following properties.

$$a_{IJ} = a_{JI}, (\text{symmetric}) \quad .$$

$$a_{IJ} = \begin{cases} 0, 1, 2, \cdots (\text{non-negative integers}) & \text{for } I \neq J \\ 0, 2, 4, \cdots (\text{non-negative even integers}) & \text{for } I = J \end{cases} \quad .$$

[5] The general tensor (9) is made of two parts: the derivative operator part and the weak-field ($h_{\lambda\rho}$) part.

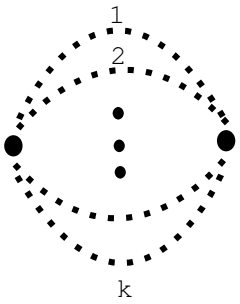

Fig.6 Two vertices are connected by k dotted lines. •-vertex represents a der-vertex or a h-vertex.

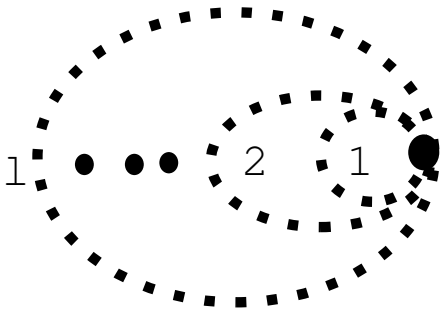

Fig.7 A vertex is connected with itself by l dotted lines. •-vertex represents a der-vertex or a h-vertex.

$$\sum_I a_{IJ} = \begin{cases} d_j & \text{for } J = j \\ & \\ 2 & \text{for } J = \bar{j} \end{cases} \quad j = 1, 2, \cdots B \quad . \tag{19}$$

The following relations can be derived from the relations (19) and the condition (8).

$$\sum_J a_{IJ} = \begin{cases} d_i & \text{for } I = i \\ & \\ 2 & \text{for } I = \bar{i} \end{cases} \quad i = 1, 2, \cdots B \quad , \quad \sum_{IJ} a_{IJ} = D + 2B \quad . \tag{20}$$

When we will soon take the relations (19) as *necessary* conditions of the adjacency matrix in its calculation algorithm (Step M2 below), the relations (20) are automatically satisfied. Because we have the freedom of naming the vertices $v_1, v_{\bar{1}}; v_2, v_{\bar{2}}; \cdots; v_B, v_{\bar{B}}$, two matrices A and A', which are related by a $2B \times 2B$ permutation matrix P in the following way, must be identified ($A \sim A'$).

$$A' \sim A \leftrightarrow A' = P^T A P \quad ,$$
$$P = \begin{pmatrix} 1 & 0 \\ 0 & 1 \end{pmatrix} \bigotimes \hat{P} \quad , \quad \hat{P} \in \text{Permutation of } (1, 2, \cdots, B) \quad , \tag{21}$$

[6]. With the above identification an adjacency matrix A can be one-to-one with a graph.

Now we summarize this section by giving the algorithm to list all independent invariants for a given D(mass dimension) and B(weak-field perturbation order, no. of bonds or h's).

Step M1 Find all possible partitions $(d_1, d_2, d_3, \cdots, d_B)$ by solving (8).

Step M2 Find all possible adjacency matrices by solving (19).

Step M3 We introduce the equivalence relation (21) among the adjacency matrices.

As a simple example, we write the adjacency matrices of P and Q which are all possible $\partial\partial h$-invariants.

$$P = \partial_\mu \partial_\mu h_{\alpha\alpha} = \text{ Graph P in Fig.3} \simeq \begin{bmatrix} 2 & 0 \\ 0 & 2 \end{bmatrix} \quad ,$$
$$Q = \partial_\alpha \partial_\beta h_{\alpha\beta} = \text{ Graph Q in Fig.3} \simeq \begin{bmatrix} 0 & 2 \\ 2 & 0 \end{bmatrix} \quad , \tag{22}$$

where $\simeq$ means that adjacency matrices are generally understood up to the freedom of (21). As the second example, we list all independent $(\partial\partial h)^2$-invariants using the adjacency matrices. $D = 4$ and $B = 2$, and the partition is $(d_1, d_2) = (2, 2)$. From

[6] In a specific case such as $d_i = d_{i'}$ $(i \neq i')$, A' coincides with A for some P's due to the presence of some same-type terms among B terms:
$\partial^{d_1} h_{\lambda_1\rho_1}, \partial^{d_2} h_{\lambda_2\rho_2}, \cdots, \partial^{d_B} h_{\lambda_B\rho_B}$.

the Step M1 to M3, we can obtain the following 13 independent representatives of adjacency matrices:

$$PP = (\partial^2 h_{\lambda\lambda})^2 \simeq \begin{bmatrix} 2 & 0 & 0 & 0 \\ 0 & 2 & 0 & 0 \\ 0 & 0 & 2 & 0 \\ 0 & 0 & 0 & 2 \end{bmatrix}, PQ = \partial^2 h_{\lambda\lambda} \cdot \partial_\mu \partial_\nu h_{\mu\nu} \simeq \begin{bmatrix} 2 & 0 & 0 & 0 \\ 0 & 2 & 0 & 0 \\ 0 & 0 & 0 & 2 \\ 0 & 0 & 2 & 0 \end{bmatrix},$$

$$C2 = \partial^2 h_{\mu\nu} \cdot \partial^2 h_{\mu\nu} \simeq \begin{bmatrix} 2 & 0 & 0 & 0 \\ 0 & 0 & 0 & 2 \\ 0 & 0 & 2 & 0 \\ 0 & 2 & 0 & 0 \end{bmatrix}, C3 = \partial_\mu \partial_\nu h_{\lambda\lambda} \cdot \partial^2 h_{\mu\nu} \simeq \begin{bmatrix} 2 & 0 & 0 & 0 \\ 0 & 0 & 2 & 0 \\ 0 & 2 & 0 & 0 \\ 0 & 0 & 0 & 2 \end{bmatrix},$$

$$C1 = \partial_\mu \partial_\nu h_{\lambda\lambda} \cdot \partial_\mu \partial_\nu h_{\sigma\sigma} \simeq \begin{bmatrix} 0 & 0 & 2 & 0 \\ 0 & 2 & 0 & 0 \\ 2 & 0 & 0 & 0 \\ 0 & 0 & 0 & 2 \end{bmatrix}, B2 = \partial^2 h_{\lambda\nu} \cdot \partial_\lambda \partial_\mu h_{\mu\nu} \simeq \begin{bmatrix} 2 & 0 & 0 & 0 \\ 0 & 0 & 1 & 1 \\ 0 & 1 & 0 & 1 \\ 0 & 1 & 1 & 0 \end{bmatrix},$$

$$B1 = \partial_\nu \partial_\lambda h_{\sigma\sigma} \cdot \partial_\lambda \partial_\mu h_{\mu\nu} \simeq \begin{bmatrix} 0 & 0 & 1 & 1 \\ 0 & 2 & 0 & 0 \\ 1 & 0 & 0 & 1 \\ 1 & 0 & 1 & 0 \end{bmatrix}, QQ = (\partial_\mu \partial_\nu h_{\mu\nu})^2 \simeq \begin{bmatrix} 0 & 2 & 0 & 0 \\ 2 & 0 & 0 & 0 \\ 0 & 0 & 0 & 2 \\ 0 & 0 & 2 & 0 \end{bmatrix},$$

$$A2 = \partial_\sigma \partial_\lambda h_{\lambda\mu} \cdot \partial_\sigma \partial_\nu h_{\mu\nu} \simeq \begin{bmatrix} 0 & 1 & 1 & 0 \\ 1 & 0 & 0 & 1 \\ 1 & 0 & 0 & 1 \\ 0 & 1 & 1 & 0 \end{bmatrix}, A3 = \partial_\sigma \partial_\lambda h_{\lambda\mu} \cdot \partial_\mu \partial_\nu h_{\nu\sigma} \simeq \begin{bmatrix} 0 & 1 & 0 & 1 \\ 1 & 0 & 1 & 0 \\ 0 & 1 & 0 & 1 \\ 1 & 0 & 1 & 0 \end{bmatrix},$$

$$B4 = \partial_\mu \partial_\nu h_{\lambda\sigma} \cdot \partial_\lambda \partial_\sigma h_{\mu\nu} \simeq \begin{bmatrix} 0 & 0 & 2 & 0 \\ 0 & 0 & 0 & 2 \\ 2 & 0 & 0 & 0 \\ 0 & 2 & 0 & 0 \end{bmatrix}, B3 = \partial_\mu \partial_\nu h_{\lambda\sigma} \cdot \partial_\mu \partial_\nu h_{\lambda\sigma} \simeq \begin{bmatrix} 0 & 0 & 0 & 2 \\ 0 & 0 & 2 & 0 \\ 0 & 2 & 0 & 0 \\ 2 & 0 & 0 & 0 \end{bmatrix},$$

$$A1 = \partial_\sigma \partial_\lambda h_{\mu\nu} \cdot \partial_\sigma \partial_\nu h_{\mu\lambda} \simeq \begin{bmatrix} 0 & 0 & 1 & 1 \\ 0 & 0 & 1 & 1 \\ 1 & 1 & 0 & 0 \\ 1 & 1 & 0 & 0 \end{bmatrix}, \tag{23}$$

where we have named the 13 invariants as above[5] and they are used in the following sections. The corresponding 13 graphs are given in the next section. In Appendix B, we list the adjacency matrices for another types of invariants: $(\partial\partial\partial h)^2$ and $(\partial\partial\partial\partial h\partial\partial h)$. They appear, for example, in the conformal anomaly calculation in the 6 dim gravity-matter theory[7].

The advantages of the adjacency matrix representation are as follows: 1) We can treat all invariants *without reference to graphs*, which allow us to do analysis in the algebraic way. This representation is powerful in some analysis of general properties of graphs[8]; 2) We can systematically treat invariants of wide-range types (cf. the graphical treatment in Sec.5). On the other hand its disadvantage is the practical difficulty of Step M3 in the algorithm. We will propose a way to resolve this point, in Sec.8, making use of the "topological" indices (introduced in Sec.7).

In Sec.3 and 4, we have presented two ways (Feynman diagram and the adjacency matrix) to cope with all invariants. Each of them is a closed formalism by itself.

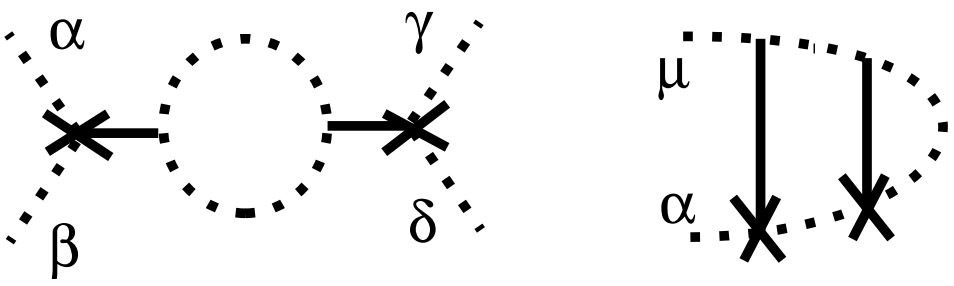

Fig.8 Graphical Representations of $\partial_\mu\partial_\nu h_{\alpha\beta}\cdot\partial_\mu\partial_\nu h_{\gamma\delta}$ and $\partial_\mu\partial_\nu h_{\alpha\beta}\cdot\partial_\nu\partial_\lambda h_{\lambda\beta}$.

In the next section we present another approach which is powerful in the practical calculation.

5 Graph Topology and List of All Invariants

From the viewpoint of the graph analysis, we present a new approach to treat invariants. For simplicity we focus on $(\partial\partial h)^s$-invariants. This type terms typically appear in the weak-field expansion of "products" of s Riemann tensors. As examples of $(\partial\partial h)^2$-tensors, we have the representations of Fig.8 for $\partial_\mu\partial_\nu h_{\alpha\beta}\partial_\mu\partial_\nu h_{\gamma\delta}$ and $\partial_\mu\partial_\nu h_{\alpha\beta}\partial_\nu\partial_\lambda h_{\lambda\beta}$. Let us state a lemma on a general SO(n)-invariant made of s $\partial\partial h$-tensors.

Lemma 2 [5] Let a general $(\partial\partial h)^s$-invariant ($s=1,2,\cdots$) has l suffix-loops. Let each loop have v_i h-vertices and w_i dd-vertices ($i=1,2,\cdots,l-1,l$). We have the following *necessary* conditions for s,l,v_i and w_i.

$$\sum_{i=1}^{l} v_i = s \quad , \quad \sum_{i=1}^{l} w_i = s \quad , \quad v_i + w_i \geq 1 \quad , \tag{24}$$
$$v_i \ , \ w_i \ = 0,1,2,\cdots \quad , \quad l = 1,2,3,\cdots,2s-1,2s \quad .$$

Here we may ignore the order of the elements in a set $\left\{ \begin{pmatrix} v_i \\ w_i \end{pmatrix} \ ; \ i=1,2,\cdots,l-1,l \right\}$ because the order can be arbitrarily changed by renumbering the suffix-loops.

This Lemma can be used to list all possible invariants.

We consider the $s=2$ case ($(\partial\partial h)^2$-invariants) in order to show how to use Lemma 2 for enumerating all invariants.

(i) $l=1$

For this case, we have

$$\begin{pmatrix} v_1 \\ w_1 \end{pmatrix} = \begin{pmatrix} 2 \\ 2 \end{pmatrix} \tag{25}$$

There are two ways to place two dd-vertices and two h-vertices on one suffix-loop. See Fig.9, where a small circle is used to represent a dd-vertex explicitly.

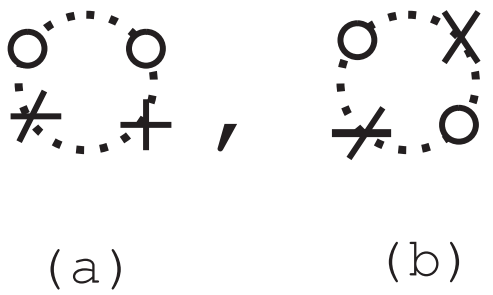

Fig.9 Two ways to place two dd-vertices (small circles) and two h-vertices (cross marks) upon one suffix-loop.

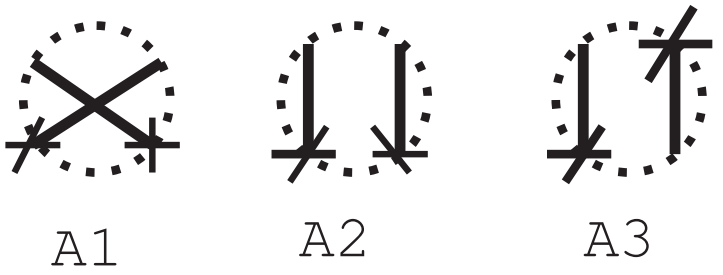

Fig.10 Three independent $(\partial\partial h)^2$-invariants for the case of one suffix-loop.

Def 4 [5] We call diagrams without bonds, like Fig.9, *bondless diagrams*.

Finally, taking account of the two bonds, we have three independent $(\partial\partial h)^2$-invariants for the case $l = 1$. We name them $A1, A2$ and $A3$ as shown in Fig.10.

(ii) $l = 2$

For this case, we have

$$\left\{\begin{pmatrix} v_1 \\ w_1 \end{pmatrix} \begin{pmatrix} v_2 \\ w_2 \end{pmatrix}\right\} = (a) : \begin{pmatrix} 2 \\ 0 \end{pmatrix} \begin{pmatrix} 0 \\ 2 \end{pmatrix} \quad , (b) : \begin{pmatrix} 1 \\ 1 \end{pmatrix} \begin{pmatrix} 1 \\ 1 \end{pmatrix} \quad , \\ (c) : \begin{pmatrix} 1 \\ 0 \end{pmatrix} \begin{pmatrix} 1 \\ 2 \end{pmatrix} \quad , (d) : \begin{pmatrix} 0 \\ 1 \end{pmatrix} \begin{pmatrix} 2 \\ 1 \end{pmatrix} \quad , \qquad (26)$$

where the order of $\begin{pmatrix} v_1 \\ w_1 \end{pmatrix}$ and $\begin{pmatrix} v_2 \\ w_2 \end{pmatrix}$ is irrelevent for the present classification as stated in Lemma 2 [7] . Each one above has one bondless diagram as shown in Fig.11. Then we have 5 independent $(\partial\partial h)^2$-invariants for this case $l = 2$. (Fig.11b has two independent ways to connect vertices by two bonds.) We name them $B1$, $B2$, $B3$, $B4$ and QQ as shown in Fig.12. Among them QQ is a *disconnected diagram*.

[7] The same treatment is adopted in the following other cases.

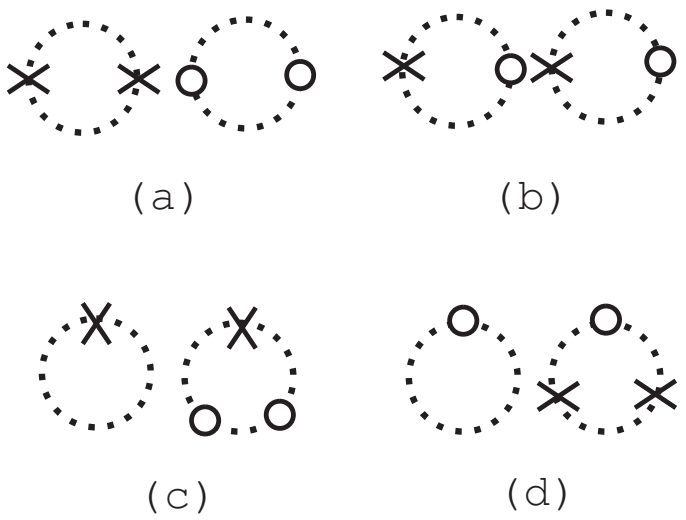

Fig.11 Bondless diagrams for (26).

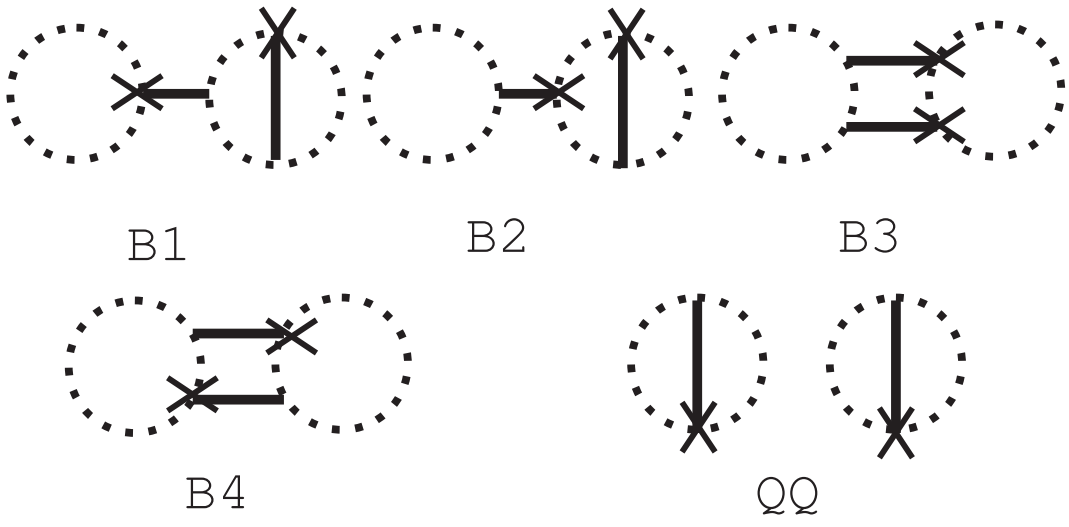

Fig.12 Five independent $(\partial\partial h)^2$-invariants for the case of two suffix-loops.

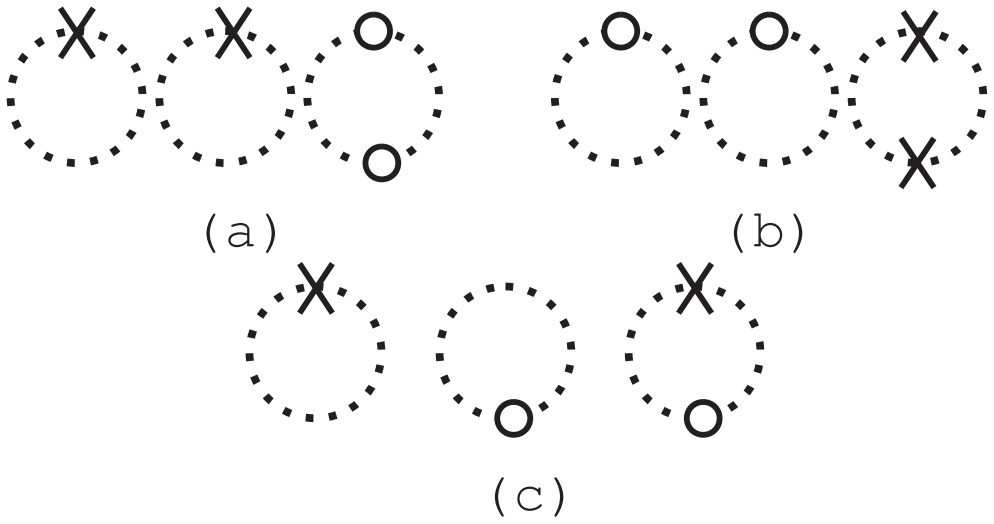

Fig.13 Three bondless diagrams corresponding to (27).

(iii) $l = 3$

For this case, we have

$$\left\{\begin{pmatrix} v_1 \\ w_1 \end{pmatrix} \begin{pmatrix} v_2 \\ w_2 \end{pmatrix} \begin{pmatrix} v_3 \\ w_3 \end{pmatrix}\right\} = (a) : \begin{pmatrix} 1 \\ 0 \end{pmatrix} \begin{pmatrix} 1 \\ 0 \end{pmatrix} \begin{pmatrix} 0 \\ 2 \end{pmatrix} \quad , \\ (b) : \begin{pmatrix} 0 \\ 1 \end{pmatrix} \begin{pmatrix} 0 \\ 1 \end{pmatrix} \begin{pmatrix} 2 \\ 0 \end{pmatrix} \quad , (c) : \begin{pmatrix} 1 \\ 0 \end{pmatrix} \begin{pmatrix} 0 \\ 1 \end{pmatrix} \begin{pmatrix} 1 \\ 1 \end{pmatrix} \quad . \tag{27}$$

Each one above has one bondless diagram as shown in Fig.13. Then we have 4 independent $(\partial\partial h)^2$-invariants for the case $l = 3$. (Fig.13c has two independent ways to connect vertices by two bonds.) We name them $C1$, $C2$, $C3$, and PQ as shown in Fig.14. Among them PQ is a disconnected diagram.

(iv) $l = 4$

For this case, we have

$$\left\{\begin{pmatrix} v_1 \\ w_1 \end{pmatrix} \begin{pmatrix} v_2 \\ w_2 \end{pmatrix} \begin{pmatrix} v_3 \\ w_3 \end{pmatrix} \begin{pmatrix} v_4 \\ w_4 \end{pmatrix}\right\} = \begin{pmatrix} 1 \\ 0 \end{pmatrix} \begin{pmatrix} 1 \\ 0 \end{pmatrix} \begin{pmatrix} 0 \\ 1 \end{pmatrix} \begin{pmatrix} 0 \\ 1 \end{pmatrix} \quad . \tag{28}$$

This corresponds to one bondless diagram shown in Fig.15. Then we have a unique independent $(\partial\partial h)^2$-invariant (disconnected) for the case $l = 4$. We name it PP as shown in Fig.16.

From (i)-(iv), we have obtained $3(l = 1)+5(l = 2)+4(l = 3)+1(l = 4)=13$ $(\partial\partial h)^2$-invariants using the *necessary* conditions (24), Lemma 2. (Among them, three ones (QQ,PQ,PP) are disconnected.) Their independence is assured by their difference of the connectivity of suffix-lines, in other words, of the *topology* of graphs. Thus we have completely listed up all independent $(\partial\partial h)^2$-invariants. The ordinary mathematical expressions for the 13 invariants will be listed in Table 1 of Sec.7. In the next section, we reprove the completeness of the above enumeration

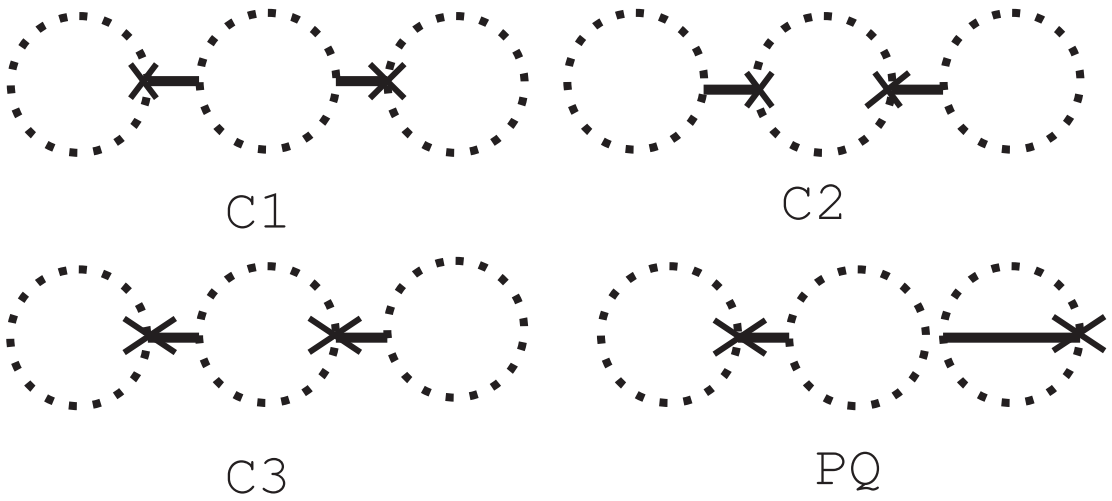

Fig.14 Four independent $(\partial\partial h)^2$-invariants for the case of three suffix-loops.

Fig.15 The bondless diagram corresponding to (28).

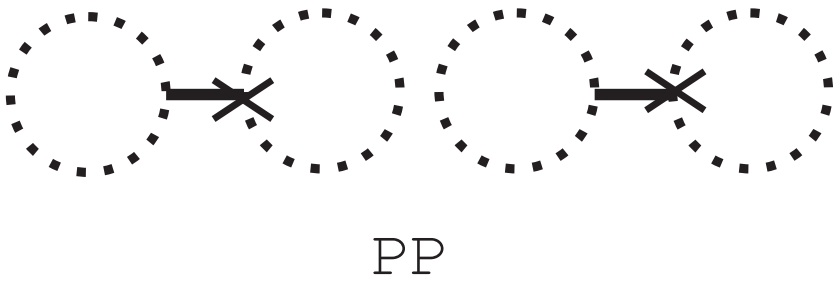

Fig.16 The unique independent $(\partial\partial h)^2$-invariant for the case of four suffix-loops.

from the standpoint of a suffix-permutation symmetry and the combinatorics among suffixes. In the similar way we can list up all independent invariants for the general type : $(\partial\partial h)^s$.

Let us summarize this section by giving the algorithm to compute all $(\partial\partial h)^s$-invariants.

Step G1 For each $l(= 1, 2, \cdots, 2s)$, obtain all possible sets of $\left\{ \begin{pmatrix} v_i \\ w_i \end{pmatrix} \ ; \ i = 1, 2, \cdots, l-1, l \right\}$ from the *necessary* condition (24).

Step G2 For each l and each set $\left\{ \begin{pmatrix} v_i \\ w_i \end{pmatrix} \ ; \ i = 1, 2, \cdots, l-1, l \right\}$, list all independent bondless diagrams.

Step G3 For each bondless diagram, list all independent graphs obtained by "placing" bonds on it in all possible ways.

6 Completeness of Graph Enumeration

Let us examine the $\partial\partial h$- and $(\partial\partial h)^2$-invariants from the viewpoint of the suffix-permutation symmetry stated below (9).

(i) $\partial\partial h$-invariants

The $\partial\partial h$-invariants are obtained by contracting 4 indices $(\mu_1, \mu_2, \mu_3, \mu_4)$ in $\partial_{\mu_1}\partial_{\mu_2}h_{\mu_3\mu_4}$. All possible ways of contracting the four indices are given by the following 3 ones.

$$a)\ \delta_{\mu_1\mu_2}\delta_{\mu_3\mu_4} \quad , \quad b)\ \delta_{\mu_1\mu_3}\delta_{\mu_2\mu_4} \quad , \quad c)\ \delta_{\mu_1\mu_4}\delta_{\mu_2\mu_3} \quad . \tag{29}$$

Due to the symmetry given below (9), we see b) and c) give the same invariant Q.

Def 5 [5] We generally call the number of occurrence of a covariant (which includes the case of an invariant) C, when contracting suffixes of a covariant C$'$ in all possible ways, a *weight* of C from C$'$.

In the present case, P has a weight 1 and Q has a weight 2 (from 4-tensor $\partial_\mu\partial_\nu h_{\alpha\beta}$). We have an identity between the number of all possible ways of suffix-contraction (29) and weights of invariants.

$$3 = 1(P) + 2(Q) \quad . \tag{30}$$

A weight of an invariant shows 'degeneracy' in the contraction due to its suffix-permutation symmetry. The above identity shows the completeness of the enumeration of $\partial\partial h$-invariants from the viewpoint of the permutation symmetry.

(ii) $(\partial\partial h)^2$-invariants

We can do the same analysis for $(\partial\partial h)^2$-invariants. The number of all possible contraction of 8 indices in the 8-tensor $\partial_{\mu_1}\partial_{\mu_2}h_{\mu_3\mu_4}\cdot\partial_{\mu_5}\partial_{\mu_6}h_{\mu_7\mu_8}$ is

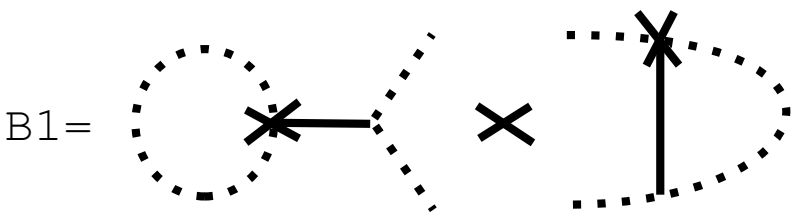

Fig.2b Fig.2c

Fig.17 Graph B1 for the weight calculation (31).

$7 \times 5 \times 3 \times 1 = 105$, from (10) with $N = 8$. Let us take $B1$ of Fig.12 as an example of weight calculation. See Fig. 17.

$$\begin{aligned} &\text{The weight of B1 from the 8-tensor} = 1(\text{weight of Fig.2b from 4-tensor } \partial\partial h) \\ &\quad \times 4(\text{weight of Fig.2c from 4-tensor } \partial\partial h) \times 2(\text{two ways of 2b-2c contraction}) \\ &\quad\quad \times 2(\text{two ways of choosing 2b-bond and 2c-bond among 2 bonds}) = 16 \quad . \end{aligned} \tag{31}$$

Similarly we can obtain weights for all other $(\partial\partial h)^2$-invariants and the following identity holds true.

$$\begin{aligned} 105 = 7 \times 5 \times 3 \times 1 &= 16(A1) + 16(A2) + 16(A3) \\ &+16(B1) + 16(B2) + 4(B3) + 4(B4) + 4(QQ) \\ &+2(C1) + 2(C2) + 4(C3) + 4(PQ) + 1(PP) \quad . \end{aligned} \tag{32}$$

This identity clearly shows the completeness of the 13 $(\partial\partial h)^2$-invariants listed in Sect.4 and 5.

Weights, defined above, correspond to the symmetry factor or the statistical factor in the Feynman diagram expansion of the field theory (Sec.3). Further the above identity (32) reminds us of a similar one, in the graph theory, called 'Polya's enumeration theorem[6].

7 Topological Indices of Graphs

The graph representation is very useful in proving mathematical properties, such as completeness and independence, of SO(n) invariants because the connectivity of suffixes can be read in the topology of a graph. In practical calculation, however, depicting graphs is cumbersome. In order to specify every graph of invariant succinctly, we introduce a set of *topological indices* which show how suffix-lines (suffixes) are connected (contracted) in a graph (an invariant). In this section we characterize every independent graph of invariant of types $\partial\partial h$ and $(\partial\partial h)^2$, by a set of some topological indices [8] .

[8] This approach is very contrasting, in the sense that they also express a graph in terms of a set of numbers, with standard ones in the graph theory: the incidence matrix or the adjacency matrix (Sec.4) [6, 8]. In Sec.8 we will present a relation to the adjacency matrix.

(i) Number of Suffix Loops ($\underline{l}$)[9]

The number of suffix loops ($\underline{l}$) of a graph is a good index. In fact, every $\partial\partial h$-invariant is completely characterized by $\underline{l}$: $\underline{l}$=2 for P and $\underline{l}$=1 for Q. The index $\underline{l}$ is not sufficient to discriminate every $(\partial\partial h)^2$-invariant. We need the following ones, (ii) and (iii).

(ii) Number of Tadpoles (tadpoleno) and Type of Tadpole (tadtype[ ])

Def 6 [5] We call a closed suffix-loop which has only one vertex, a *tadpole*. The number of tadpoles which a graph has, is called *tadpole number* (tadpoleno) of the graph. Let us consider t-th tadpole in a graph ($t = 1, 2, \cdots$,tadpoleno). When the vertex which the t-th tadpole has, is dd-vertex (h-vertex) its *tadpole type*, tadtype[t], is defined to be 0 (1). tadtype[ ] is assigned for each tadpole.

For example, in Fig.3, P has tadpoleno=2 and tadtype[1]=0 and tadtype[2]=1. [10] Q has tadpoleno=0.

(iii) Bond Changing Number(bcn[ ]) and Vertex Changing Number(vcn[ ])

Def 7 [5] bcn[k] and vcn[k] are defined for k-th suffix-loop ($k = 1, 2, \cdots, \underline{l}$) as follows. When we trace a suffix-loop, starting from a vertex in a certain direction, we generally pass some vertices, and finally come back to the starting vertex. See Fig.18. When we move, in the tracing, from a vertex to a next vertex, we compare the bonds to which the two vertices belong, and their vertex-types. If the bonds are different, we set $\Delta\underline{\text{bcn}} = 1$, otherwise $\Delta\underline{\text{bcn}} = 0$, If the vertex-types are different, we set $\Delta\underline{\text{vcn}} = 1$, otherwise $\Delta\underline{\text{vcn}} = 0$. For k-th loop, we sum every number of $\Delta\underline{\text{bcn}}$ and $\Delta\underline{\text{vcn}}$ while tracing the loop once, and assign as $\sum_{\text{along } k\text{-th loop}} \Delta\underline{\text{bcn}} \equiv \underline{\text{bcn}}[k]$, $\sum_{\text{along } k\text{-th loop}} \Delta\underline{\text{vcn}} \equiv \underline{\text{vcn}}[k]$. [11]

A practical way to calculate bcn[ ] and vcn[ ] is explained in Appendix C.

In Table 1, we list all indices necessary for discriminating every $(\partial\partial h)^2$-invariant completely. The listed 13 invariants are independent each other because Table 1 clearly shows the topology of every graph is different.

[9] All indices are underlined. For example, $\underline{l}$, tadpoleno, tadtype, bcn, and vcn.

[10] Final results should be independent of arbitrariness in numbering all tadpoles in a graph.

[11] Final results should be independent of arbitrariness of numbering all suffix-loops in a graph.

Graph \ Indices	l	tadpoleno	tadtype[ ]	bcn[ ]	vcn[ ]
$A1 = \partial_\sigma\partial_\lambda h_{\mu\nu} \cdot \partial_\sigma\partial_\nu h_{\mu\lambda}$	1	0	nothing	4	2
$A2 = \partial_\sigma\partial_\lambda h_{\lambda\mu} \cdot \partial_\sigma\partial_\nu h_{\mu\nu}$	1	0	nothing	2	2
$A3 = \partial_\sigma\partial_\lambda h_{\lambda\mu} \cdot \partial_\mu\partial_\nu h_{\nu\sigma}$	1	0	nothing	2	4
$B1 = \partial_\nu\partial_\lambda h_{\sigma\sigma} \cdot \partial_\lambda\partial_\mu h_{\mu\nu}$	2	1	1	/	/
$B2 = \partial^2 h_{\lambda\nu} \cdot \partial_\lambda\partial_\mu h_{\mu\nu}$	2	1	0	/	/
$B3 = \partial_\mu\partial_\nu h_{\lambda\sigma} \cdot \partial_\mu\partial_\nu h_{\lambda\sigma}$	2	0	nothing	2 2	0 0
$B4 = \partial_\mu\partial_\nu h_{\lambda\sigma} \cdot \partial_\lambda\partial_\sigma h_{\mu\nu}$	2	0	nothing	2 2	2 2
$Q^2 = (\partial_\mu\partial_\nu h_{\mu\nu})^2$	2	0	nothing	0 0	2 2
$C1 = \partial_\mu\partial_\nu h_{\lambda\lambda} \cdot \partial_\mu\partial_\nu h_{\sigma\sigma}$	3	2	1 1	/	/
$C2 = \partial^2 h_{\mu\nu} \cdot \partial^2 h_{\mu\nu}$	3	2	0 0	/	/
$C3 = \partial_\mu\partial_\nu h_{\lambda\lambda} \cdot \partial^2 h_{\mu\nu}$	3	2	1 0	0 0 2	0 0 2
$PQ = \partial^2 h_{\lambda\lambda} \cdot \partial_\mu\partial_\nu h_{\mu\nu}$	3	2	1 0	0 0 0	0 0 2
$P^2 = (\partial^2 h_{\lambda\lambda})^2$	4	/	/	/	/

Table 1 List of indices for all $(\partial\partial h)^2$-invariants. The symbol '/' means 'need not be calculated for discrimination'.

We have presented the set of indices which is sufficient to discriminate all $\partial\partial h$-

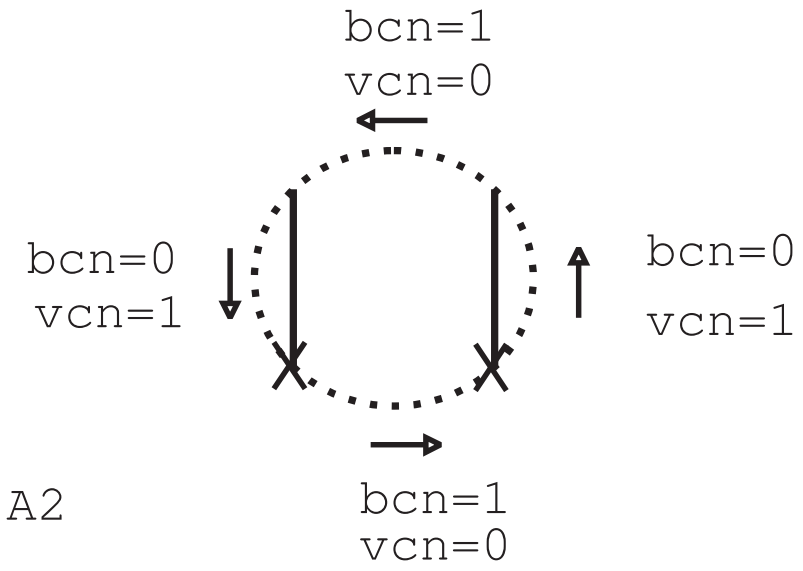

Fig.18 Explanation of bcn[ ] and vcn[ ] using Graph A2.

and $(\partial\partial h)^2$-invariants. For the case of $(\partial\partial h)^3$-invariants, see Ref.[5]. It is a non-trivial work to find an appropriate set of indices for higher-order invariants. However, once the set of indices is fixed, the computation itself is very efficient and is most appropriate for the computer algorithm[9]. These advatageous and disadvatageous points should be compared with the case of the adjacency matrix. In Sec.8, we will explain how to read the indices from the adjacency matrix.

8 Calculation of Indices from Adjacency Matrices

In Sec.4 we have introduced the adjacency matrix to represent a graph. As shown in Step M3, there exist some equivalent matrices which express the same graph due to the arbitrariness of vertex-naming. It is very hard (at least practically) to find the permutation P in (21) and identify a representative. In this section, we explain how to read the topological indices of a graph from the matrix: $A = [a_{IJ}]$; $I, J = 1, \bar{1}, 2, \bar{2}, \cdots, B, \bar{B}$. It is useful when we efficiently identify an invariant (a representative) in the matrix representation.

(i) Number of Tadpoles (tadpoleno) and Type of Tadpole (tadtype[ ])
These two indices can be most easily read from the matrix.

$$\underline{\text{tadpoleno}} = \frac{1}{2}\sum_I a_{II} = \frac{1}{2}\ \text{Trace}\ A\ ,\ \ I = 1, \bar{1}, 2, \bar{2}, \cdots, B, \bar{B} \quad .$$

$$\underline{\text{tadtype}}[\text{t}] = \begin{cases} 0\ \text{(der-vertex)} & \text{for } I = i\ ,\ a_{II} \neq 0 \\ 1\ \text{(h-vertex)} & \text{for } I = \bar{i}\ ,\ a_{II} \neq 0 \end{cases} \quad ,$$

$$t = 1, 2, \cdots, \underline{\text{tadpoleno}} \quad . \tag{33}$$

As example, for $C3$ of (23) we have

$$\begin{aligned} \underline{\text{tadpoleno}} &= \frac{1}{2}(2+0+0+2) = 2 \quad , \\ \underline{\text{tadtype}}[1] &= 0 \ (\ a_{11} = 2\ ) \quad , \\ \underline{\text{tadtype}}[2] &= 1 \ (\ a_{\bar{2}\bar{2}} = 2\ ) \quad , \end{aligned} \tag{34}$$

which are same as shown in Table 1.

(ii) $\underline{\text{connectivity}}$
First we define a new index *connectivity*.

Def 8 [5] Let us consider a graph of invariants with s bonds. There are ${}_sC_2 = s(s-1)/2$ different pairs of bonds. We define $\underline{\text{connectivity}}$ of the graph as the total number of those pairs which are connected by at least one suffix-line. $0 \leq \underline{\text{connectivity}} \leq s(s-1)/2$.

This new index is one of important indices in the calculation of the $(\partial\partial h)^3$-invariants [5]. An adjacency matrix with the size of $2B \times 2B$ is composed of B^2 submatrices B_{ij} with the size of 2×2. Then the connectivity is obtained by

$$\begin{aligned} \underline{\text{connectivity}} &= \tfrac{1}{2}\{\ \text{No. of off-diagonal}(i \neq j)\ \text{non-empty elements}\ B_{ij}\ \text{in}\ A = (B_{ij})\ \}\ , \\ B_{ij} &\equiv \begin{bmatrix} a_{ij} & a_{i\bar{j}} \\ a_{\bar{i}j} & a_{\bar{i}\bar{j}} \end{bmatrix} = (B_{ji})^T \quad , \end{aligned} \tag{35}$$

where "empty" ("non-empty") means ${a_{ij}}^2 + {a_{i\bar{j}}}^2 + {a_{\bar{i}j}}^2 + {a_{\bar{i}\bar{j}}}^2 = (\neq)0$. When B_{ij} is empty, it means i-th bond and j-th bond are not connected by any suffix-lines. We give an example.

$$G9 \equiv \partial_\mu\partial_\omega h_{\mu\nu} \cdot \partial_\nu\partial_\lambda h_{\tau\sigma} \cdot \partial_\lambda\partial_\sigma h_{\tau\omega} = \text{Fig.19} = \begin{bmatrix} 0 & 0 & 1 & 1 & 0 & 0 \\ 0 & 0 & 0 & 1 & 1 & 0 \\ 1 & 0 & 0 & 0 & 0 & 1 \\ 1 & 1 & 0 & 0 & 0 & 0 \\ 0 & 1 & 0 & 0 & 0 & 1 \\ 0 & 0 & 1 & 0 & 1 & 0 \end{bmatrix} \quad ,$$

$$B_{12}\ ,\ B_{23}\ ,\ B_{31}\ ,\ B_{21} = {B_{12}}^T\ ,\ B_{32} = {B_{23}}^T \text{ and } B_{13} = {B_{31}}^T \text{ are non-empty} \quad ,$$

$$\underline{\text{connectivity}} = \frac{1}{2} \times 6 = 3 \quad . \tag{36}$$

$\underline{\text{disconnectivity}}$ is defined in Ref.[5] and can be calculated from adjacency matrices in the similar way.

(iii) Number of Suffix Loops ($\underline{l}$)

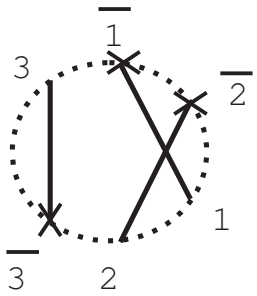

Fig.19 Graph G9$\equiv \partial_\mu\partial_\omega h_{\mu\nu}\cdot\partial_\nu\partial_\lambda h_{\tau\sigma}\cdot\partial_\lambda\partial_\sigma h_{\tau\omega}$.

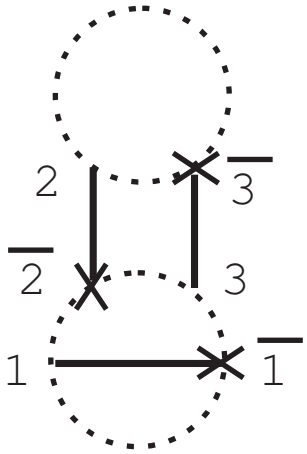

Fig.20 Graph of G25$\equiv \partial_\mu\partial_\nu h_{\lambda\sigma}\cdot\partial_\sigma\partial_\tau h_{\mu\nu}\cdot\partial_\lambda\partial_\omega h_{\tau\omega}$.

There are several important indices associated with a suffix-loop. Therefore it is the first important thing to find every independent suffix-loop in an adjacency matrix. Let us explain it with an example.

$$G25\equiv\partial_\mu\partial_\nu h_{\lambda\sigma}\cdot\partial_\sigma\partial_\tau h_{\mu\nu}\cdot\partial_\lambda\partial_\omega h_{\tau\omega}=\text{Fig.20}=\begin{bmatrix}0 & 1_a & 0 & 1_{d'} & 0 & 0\\ 1_{a'} & 0 & 0 & 0 & 1_b & 0\\ 0 & 0 & 0 & 0 & 0 & 2_{e,f'}\\ 1_d & 0 & 0 & 0 & 1_{c'} & 0\\ 0 & 1_{b'} & 0 & 1_c & 0 & 0\\ 0 & 0 & 2_{f,e'} & 0 & 0 & 0\end{bmatrix} \quad .(37)$$

We see two independent suffix-loops,$\underline{l}$=2 : [loop1] $a-b-c-d-a$; [loop2] $e-f-e$. The remaining two loops, $a'-b'-c'-d'-a'$ and $e'-f'-e'$, are the symmetric copies of loop1 and loop2 respectively. (loop2 and its copy overlap in the matrix.) To systematically find suffix-loops in a finite-size matrix in general is

easy (by use of a computer) as far as the size is not so large. It is done by searching closed loops of "successive" (row,column)-numbers of the adjacency matrix.

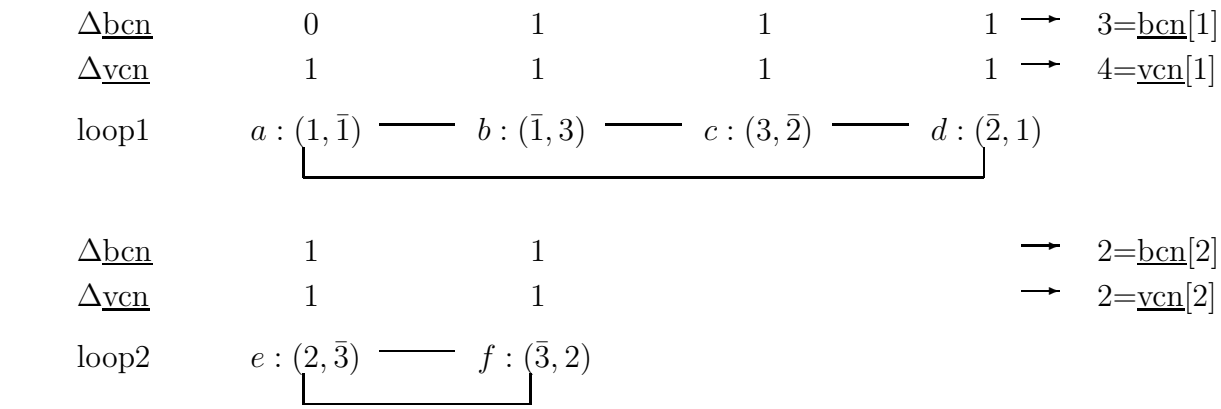

The numbers associated with $\Delta\underline{\text{bcn}}$ and $\Delta\underline{\text{vcn}}$, in the above illustration, is used in the next item.

(iv) Bond Changing Number($\underline{\text{bcn}}[\,]$) and Vertex Changing Number($\underline{\text{vcn}}[\,]$)

When a suffix-loop, which is named l-th loop, is given in the form of a series of (row, column)-numbers of an adjacency matrix, as given in iii), $\Delta\underline{\text{bcn}}$ and $\Delta\underline{\text{vcn}}$ are immediately given by as follows.

$$\text{For an element (row}=I\text{,column}=J\text{) in the } l\text{-th loop}$$

$$\Delta\underline{\text{bcn}} = \begin{cases} 0 & \text{for } i = j \\ 1 & \text{for } i \neq j \end{cases} ,$$

$$\Delta\underline{\text{vcn}} = \begin{cases} 0 & \text{for } (I = i, J = j) \text{ or } (I = \bar{i}, J = \bar{j}) \\ 1 & \text{for } (I = i, J = \bar{j}) \text{ or } (I = \bar{i}, J = j) \end{cases} . \qquad (38)$$

The total sums of $\Delta\underline{\text{bcn}}$ and $\Delta\underline{\text{vcn}}$ along the l-th loop give $\underline{\text{bcn}}[l]$ and $\underline{\text{vcn}}[l]$ respectively. An example is given in iii).

Another interesting index $\underline{\text{bridgeno}}$ is defined and is related to the adjacency matrix in App. B.

9 Application to Gravitational Theories

Let us apply the obtained result to some simple problems. First the weak-field expansion of Riemann tensors are graphically represented as in Fig.21. Using them, general invariants with the mass dimension $(\text{Mass})^4$ are expanded and their $(\partial\partial h)^2$-parts are given in Table 2.

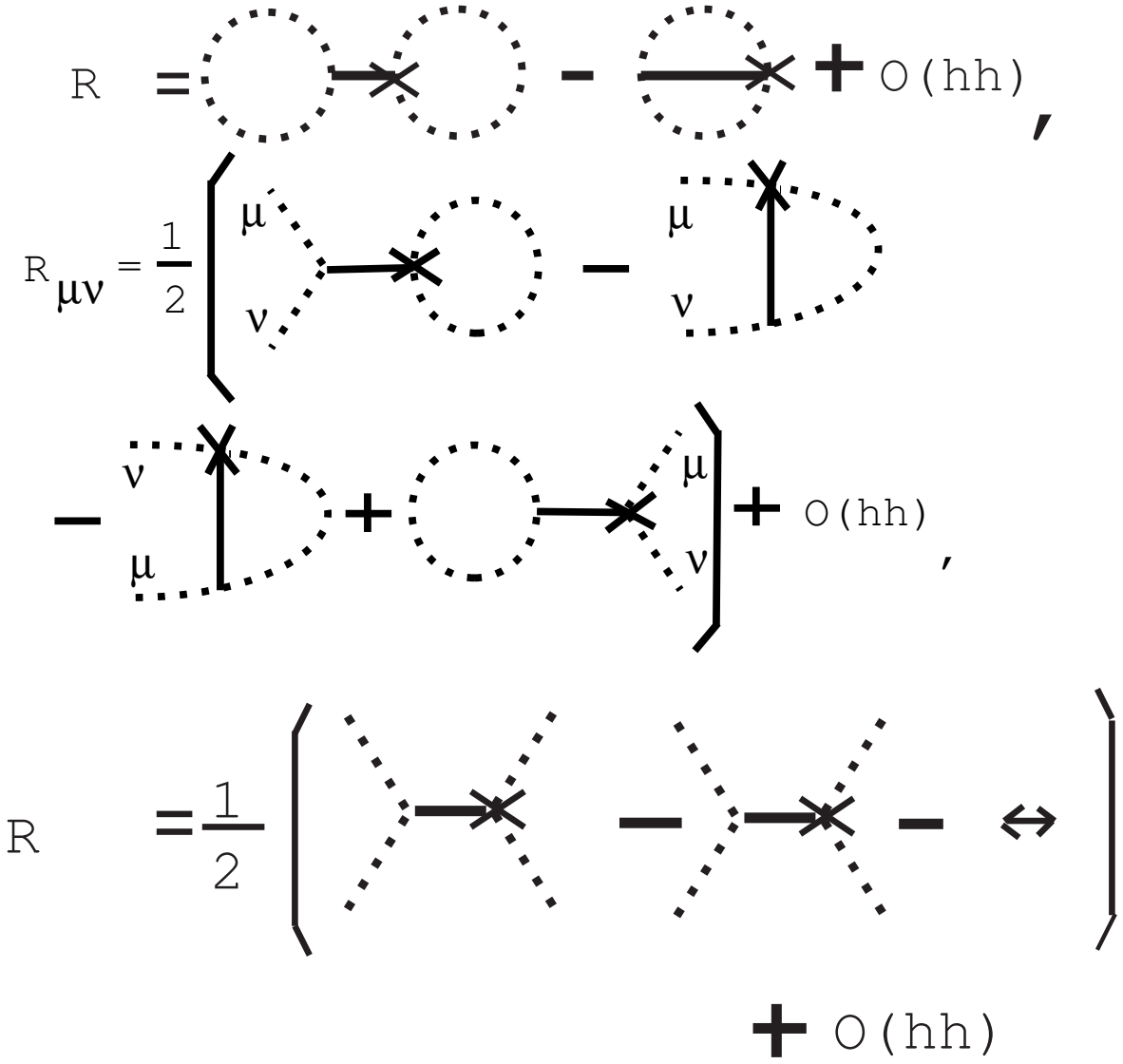

Fig.21 Graphical representation of weak expansion of Riemann tensors .

Graph	$\nabla^2 R$	R^2	$R_{\mu\nu}R^{\mu\nu}$	$R_{\mu\nu\lambda\sigma}R^{\mu\nu\lambda\sigma}$
$A1$	1	0	0	-2
$A2$	2	0	$\frac{1}{2}$	0
$A3$	0	0	$\frac{1}{2}$	0
$B1$	-2	0	-1	0
$B2$	2	0	-1	0
$B3$	$-\frac{3}{2}$	0	0	1
$B4$	0	0	0	1
Q^2	0	1	0	0
$C1$	$\frac{1}{2}$	0	$\frac{1}{4}$	0
$C2$	-1	0	$\frac{1}{4}$	0
$C3$	-1	0	$\frac{1}{2}$	0
PQ	0	-2	0	0
P^2	0	1	0	0

Table 2 Weak-Expansion of Invariants with (Mass)^4-Dim. : $(\partial\partial h)^2$-Part

The four invariants, $\nabla^2 R$, R^2 , $R_{\mu\nu}R^{\mu\nu}$ and $R_{\mu\nu\lambda\sigma}R^{\mu\nu\lambda\sigma}$, are important in the Weyl anomaly calculation[10, 11] and (1-loop) counter term calculation in 4 dim quantum gravity[12, 13]. From the explicit result of Table 2, we see the four invariants are independent as local functions of $h_{\mu\nu}(x)$, because the 13 $(\partial\partial h)^2$-invariants are independent each other. In particular, the three 'products' of Riemann tensors (R^2 , $R_{\mu\nu}R^{\mu\nu}$, $R_{\mu\nu\lambda\sigma}R^{\mu\nu\lambda\sigma}$) are 'orthogonal', at the leading order of weak field perturbation, in the space 'spanned' by the 13 $(\partial\partial h)^2$-invariants. Note here that the independence of the four invariants is proven for a general metric $g_{\mu\nu} = \delta_{\mu\nu} + h_{\mu\nu}$. As for the next higher mass dimension case, (Mass)^6 general invariants, it has been shown that, in the same way as above, the following 17 ones are complete and independent[5].

$$
\begin{aligned}
P_1 = RRR \quad , \; P_2 = RR_{\mu\nu}R^{\mu\nu} \quad , \; P_3 = RR_{\mu\nu\lambda\sigma}R^{\mu\nu\lambda\sigma} \quad , \\
P_4 = R_{\mu\nu}R^{\nu\lambda}R_{\lambda}{}^{\mu} \quad , \; P_5 = -R_{\mu\nu\lambda\sigma}R^{\mu\lambda}R^{\nu\sigma} \quad , \; P_6 = R_{\mu\nu\lambda\sigma}R_{\tau}{}^{\nu\lambda\sigma}R^{\mu\tau} \quad , \\
A_1 = R_{\mu\nu\lambda\sigma}R^{\sigma\lambda}{}_{\tau\omega}R^{\omega\tau\nu\mu} \quad , \; B_1 = R_{\mu\nu\tau\sigma}R^{\nu}{}_{\lambda\omega}{}^{\tau}R^{\lambda\mu\sigma\omega} \quad , \\
O_1 = \nabla^{\mu}R \cdot \nabla_{\mu}R \quad , \; O_2 = \nabla^{\mu}R_{\lambda\sigma} \cdot \nabla_{\mu}R^{\lambda\sigma} \quad , \\
O_3 = \nabla^{\mu}R^{\lambda\rho\sigma\tau} \cdot \nabla_{\mu}R_{\lambda\rho\sigma\tau} \quad , \; O_4 = \nabla^{\mu}R_{\lambda\nu} \cdot \nabla^{\nu}R^{\lambda}{}_{\mu} \quad , \\
T_1 = \nabla^2 R \cdot R \quad , \; T_2 = \nabla^2 R_{\lambda\sigma} \cdot R^{\lambda\sigma} \quad , \; T_3 = \nabla^2 R_{\lambda\rho\sigma\tau} \cdot R^{\lambda\rho\sigma\tau} \quad , \\
T_4 = \nabla^{\mu}\nabla^{\nu}R \cdot R_{\mu\nu} \quad , \\
S = \nabla^2\nabla^2 R \quad . \qquad (39)
\end{aligned}
$$

We consider, as the next application, the Weyl anomalies for the gravity-matter theory in "diverse" dimensions. Anomaly formulae are obtained in Ref.[11]. Its lowest non-trivial order, w.r.t. the weak-field, in n-dim space is given by the t^0-part of the trace of the following formula.

$$
G_1(x, y; t) = \int d^n z \int_0^t ds G_0(x - z; t - s)\vec{V}(z)G_0(z - y; s) \quad ,
$$

$$G_0(x;t) = \frac{1}{(4\pi t)^{n/2}} e^{-\frac{x^2}{4t}}\ I_N \quad , \tag{40}$$

where $\vec{V}(z)$ is the interaction part of the system (elliptic) operator, I_N is the $N \times N$ unit matrix (N: the number of matter-field components). $G_0(x;t)$ is the solution of the n-dim heat equation with the temperature t. As the simplest model, we take the conformal invariant gravity-scalar theory ($N = 1$) in n-dim space.

$$\mathcal{L} = \sqrt{g}(\frac{1}{2}\nabla_\mu\phi\nabla^\mu\phi - \frac{n-2}{8(n-1)}R\phi^2) \quad , \tag{41}$$

Then the operator $\vec{V}(z)$ is, at the lowest order, given by (see eq.(16) of Ref.[11])

$$\begin{aligned} \vec{V} &= W_{\mu\nu}\partial_\mu\partial_\nu + N_\mu\partial_\mu + M \quad , \\ W_{\mu\nu} = -h_{\mu\nu} + O(h^2) \quad &, \quad N_\lambda = -\partial_\mu h_{\lambda\mu} + O(h^2) \quad , \\ M = \frac{n-2}{4(n-1)}(\partial^2 h - \partial_\alpha\partial_\beta h_{\alpha\beta}) &- \frac{1}{4}\partial^2 h + O(h^2) \quad . \end{aligned} \tag{42}$$

The diagonal ($x = y$) part, $G_1(x,x;t)$, finally reduces to

$$\begin{aligned} G_1(x,x;t) &= \frac{1}{(4\pi)^{n/2}t^{(n/2)-1}} \int d^n w \int_0^1 dr G_0(w;(1-r)r) \\ \times[\frac{1}{t}W_{\mu\nu}(x+\sqrt{t}w)(-\frac{\delta_{\mu\nu}}{2r} + \frac{w_\mu w_\nu}{4r^2}) &+ \frac{1}{\sqrt{t}}N_\mu(x+\sqrt{t}w)(-\frac{w_\mu}{2r}) + M(x+\sqrt{t}w)] \ . \end{aligned} \tag{43}$$

Taylor-expanding $W_{\mu\nu}, N_\mu$ and M in the above expression w.r.t. small t, and the t^0-part of G_1 gives the lowest order of the Weyl anomaly terms. For various dimensions, relevant terms are graphically shown in Fig.22. The general invariant forms are obtained as follows.

$$\begin{aligned} 2 \text{ dim } : \quad A_2 &= \tfrac{1}{4\pi}\sqrt{g}\{-\tfrac{1}{6}R\} \ , \\ 4 \text{ dim } : \quad A_4 &= \tfrac{1}{(4\pi)^2}\sqrt{g}\{-\tfrac{1}{180}\nabla^2 R + (RR - \text{terms})\} \ , \\ 6 \text{ dim } : \quad A_6 &= \tfrac{1}{(4\pi)^3}\sqrt{g}\{-\tfrac{1}{4200}\nabla^4 R + (\nabla\nabla RR-, RRR - \text{terms})\} \ , \\ 8 \text{ dim } : \quad A_8 &= \tfrac{1}{(4\pi)^4}\sqrt{g}\{-\tfrac{1}{7!\cdot 2}\nabla^6 R \\ &\quad +(\nabla\nabla\nabla\nabla RR-, \nabla\nabla RRR-, RRRR - \text{terms})\} \ , \\ 10 \text{ dim } : \quad A_{10} &= \tfrac{1}{(4\pi)^5}\sqrt{g}\{-\tfrac{4}{9!\cdot 33}\nabla^8 R \\ +(\nabla\nabla\nabla\nabla\nabla\nabla RR-, \nabla\nabla\nabla\nabla RRR-, &\nabla\nabla RRRR-, RRRRR - \text{terms})\} \ . \end{aligned} \tag{44}$$

The omitted part of ($\cdots$-terms) is given by the higher-order calculation. The full form is well-established up to A_4.

10 Conclusions and Discussions

We have presented a graphical representation of global SO(n) tensors. This approach allows us to systematically list all and independent SO(n) invariants. We have proposed some new methods for it: the adjacency matrices, the Feynman

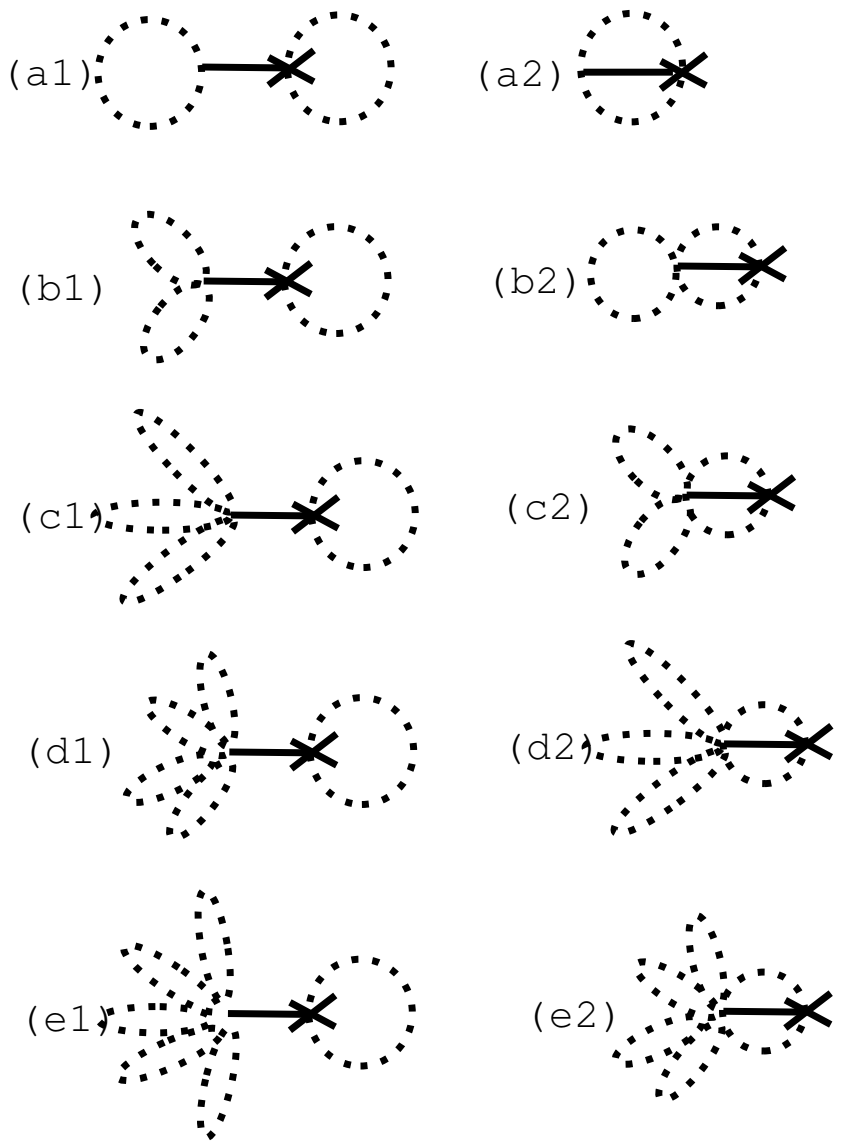

Fig.22 Lowest order graphs for the Weyl anomaly calculation (44):

[2 dim] (a1) $\partial^2 h \simeq \begin{bmatrix} 2 & 0 \\ 0 & 2 \end{bmatrix}$, (a2) $\partial_\mu \partial_\nu h_{\mu\nu} \simeq \begin{bmatrix} 0 & 2 \\ 2 & 0 \end{bmatrix}$;

[4 dim] (b1) $(\partial^2)^2 h \simeq \begin{bmatrix} 4 & 0 \\ 0 & 2 \end{bmatrix}$, (b2) $\partial^2 \partial_\mu \partial_\nu h_{\mu\nu} \simeq \begin{bmatrix} 2 & 2 \\ 2 & 0 \end{bmatrix}$;

[6 dim] (c1) $(\partial^2)^3 h \simeq \begin{bmatrix} 6 & 0 \\ 0 & 2 \end{bmatrix}$, (c2) $(\partial^2)^2 \partial_\mu \partial_\nu h_{\mu\nu} \simeq \begin{bmatrix} 4 & 2 \\ 2 & 0 \end{bmatrix}$;

[8 dim] (d1) $(\partial^2)^4 h \simeq \begin{bmatrix} 8 & 0 \\ 0 & 2 \end{bmatrix}$, (d2) $(\partial^2)^3 \partial_\mu \partial_\nu h_{\mu\nu} \simeq \begin{bmatrix} 6 & 2 \\ 2 & 0 \end{bmatrix}$;

[10 dim] (e1) $(\partial^2)^5 h \simeq \begin{bmatrix} 10 & 0 \\ 0 & 2 \end{bmatrix}$, (e2) $(\partial^2)^4 \partial_\mu \partial_\nu h_{\mu\nu} \simeq \begin{bmatrix} 8 & 2 \\ 2 & 0 \end{bmatrix}$.

diagrams, the topological index method, etc.. They all give a consistent result, but each of them has its advantageous and disadvantageous points. We can apply them to any higher order invariants in principle [12] . As some simple examples, we have calculated all $\partial\partial h-, (\partial\partial h)^2-, (\partial\partial\partial h)^2-$ and $(\partial\partial h)(\partial\partial\partial h)-$ invariants. The completeness of the list is reassured by an identity between a combinatoric number of suffixes and weights of listed terms due to their suffix-permutation symmetries. Some topological indices, sufficient for discriminating all $\partial\partial h$- and $(\partial\partial h)^2$-invariants, are given. They are useful in practical (computer) calculation. Finally we have applied the result to some problems in the general relativity.

The present graphical representation for global SO(n) tensors is complementary to that for general tensors given in [14]. The latter one deals with general covariants, and its results are independent of the perturbation. In the general covariant representation, however, it is difficult to prove the independence of listed general invariants because there is no independent 'bases'. On the other hand, in the present case, although the analysis is based on the weak field perturbation, we have independent 'bases' (like 13 $(\partial\partial h)^2$- invariants) at each perturbation order. It allows us to prove independence of listed general invariants. The independence of R^3-type general invariants is shown, using the present approach, in Ref.[5].

Stimulated by the string theory, the importance of physics in the higher dimensions is increasing. Especially $n = 10$ dimensions is the critical one. When the string physics is so well developed that the dynamical aspect becomes clearer, we suppose that the relation between the string field theory and the ordinary field theory becomes seriously important. At present no consistent field heory in higher than 4 dim is known except the "free" theories like (41). We believe the present result gives some useful tools for such analysis. For example we must treat $(\partial\partial h)^5$-invariants, like terms graphically shown in Fig.23, in order to completely determine A_{10}.

Some results such as (32) and Table 2 are obtained or checked by the computer calculation using a C-language program [9].

Acknowledgement

The authors thank Prof.K.Murota (RIMS,Kyoto Univ.) for discussions and comments about the present work. They express gratitude to Prof. N.Nakanishi

[12] The present analysis reduces the problem to the two key points: a) classification of the higher order SO(n)-invariants; b) computer program and calculation. The point b) is purely a technical problem. Rough estimation shows the Weyl anomaly calculation, for example, in 10 dim is possible at the present middle-size workstation.

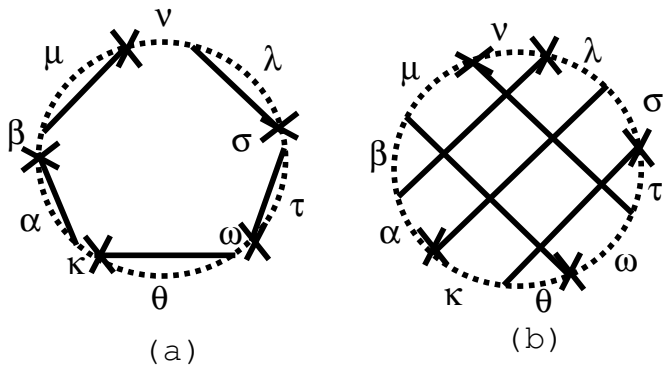

Fig.23 (a) $\partial_\alpha\partial_\kappa h_{\alpha\beta}\cdot\partial_\beta\partial_\mu h_{\mu\nu}\cdot\partial_\nu\partial_\lambda h_{\lambda\sigma}\cdot\partial_\sigma\partial_\tau h_{\tau\omega}\cdot\partial_\omega\partial_\theta h_{\theta\kappa}$ and (b) $\partial_\tau\partial_\omega h_{\mu\nu}\cdot\partial_\mu\partial_\beta h_{\omega\theta}\cdot\partial_\alpha\partial_\beta h_{\nu\lambda}\cdot\partial_\lambda\partial_\sigma h_{\alpha\kappa}\cdot\partial_\kappa\partial_\theta h_{\sigma\tau}$.

and Prof. K.Murota for reading the initial version of the manuscript carefully.

Appendix A. The Young Tableaus

We can calculate $SO(n)$ invariants by the Young diagram method. The general theories are discussed in [3] and [4]. So we briefly explain this method taking simple examples: $\partial\partial h$- and $(\partial\partial h)^2$- invariants.

The permutation symmetries w.r.t. the indices in a term, $\partial_{\mu_1}\cdots\partial_{\mu_d}h_{\lambda\rho}$, are represented by the following Young tableaus:

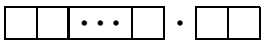

where the first tableau has d boxes in a row and "$\cdot$" is the product of the Young tableaus. We simply express the above diagram by a symbol arranging the box numbers of each row, so the term $\partial_{\mu_1}\cdots\partial_{\mu_d}h_{\lambda\rho}$ is expressed as $\{d\}\cdot\{2\}$.

$\partial_\mu\partial_\nu h_{\lambda\rho}$ is decomposed as

$$\{2\}\cdot\{2\}=\{4\}+\{31\}+\{22\},$$

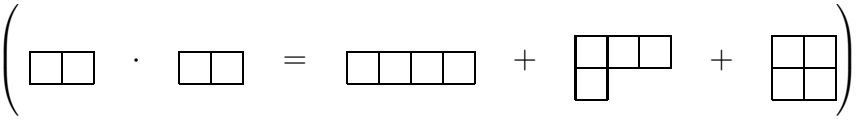

(45)

by the Littlewood-Richardson rule to obtain irreducible representations of the symmetric groups. The right hand side of (45) corresponds to the independent symmetrizations or antisymmetrizations of indices in $\partial_\mu\partial_\nu h_{\lambda\rho}$. We contract the indices and obtain $SO(n)$ invariants. One tableau can produce one independent invariant. The contraction, however, gives a non-zero result only when all the box

numbers of each row are even. Therefore in the above $\partial\partial h$ example, we obtain only two independent invariants from $\{4\}$ and $\{22\}$.

$$\begin{array}{|c|c|c|c|}\hline \mu & \nu & \lambda & \sigma \\ \hline \end{array} \times\ \delta_{\mu\nu}\delta_{\lambda\sigma} \qquad \propto \quad P+Q \quad ,$$

$$\begin{array}{|c|c|}\hline \mu & \nu \\ \hline \lambda & \sigma \\ \hline \end{array} \times\ \delta_{\mu\nu}\delta_{\lambda\sigma} \qquad \propto \quad P-Q \quad , \tag{46}$$

where $P \equiv \partial_\mu\partial_\mu h_{\nu\nu}$ and $Q \equiv \partial_\mu\partial_\nu h_{\mu\nu}$ are defined in the text. Generally, the independent invariants are obtained from the tableaus whose box numbers of each row are all even.

However when we calculate the independent invariants from the products of the *same* tensors, we must modify the Littlewood-Richardson rule to obtain the appropriate ones. The Young tableaus to obtain the irreducible representations of the symmetric groups does not produce the correct results in such case. For example, $(\partial\partial h)^2$ invariants are not the decomposition of

$$(\{4\}+\{31\}+\{22\})\cdot(\{4\}+\{31\}+\{22\}). \tag{47}$$

In order to symmetrize the products, we use the 'plethysm' operation $\otimes$, which is explained in the appendix in [3]. Since it is the rather complicated theory, we do not explain it in this paper. We represent $(\partial\partial h)^2$ invariants as

$$(\{4\}+\{31\}+\{22\})^{\otimes\{2\}}, \tag{48}$$

and they are calculated by the plethysm method as

$$\begin{aligned}(\{2\}\cdot\{2\})^{\otimes\{2\}} &= (\{4\}+\{31\}+\{22\})^{\otimes\{2\}} \\ &= \{4\}^{\otimes\{2\}}+\{31\}^{\otimes\{2\}}+\{22\}^{\otimes\{2\}}+\{4\}\{31\} \\ &\quad +\{4\}\{22\}+\{31\}\{22\} \\ &= \{8\}+4\{62\}+3\{44\}+4\{422\}+\{2222\}+\text{uneven terms}\end{aligned} \tag{49}$$

$=$ 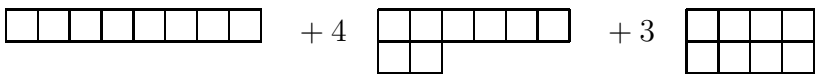 $+4$ $+3$

$+4$ 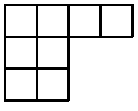 $+$ 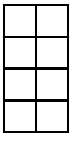 $+$ uneven terms,

where the numbers in front of Young tableaus above show those of independent representations of the same type. The 13 independent Young Tableaus give, after contraction, the 13 independent $(\partial\partial h)^2$-invariants, which are the linear combinations of 13 terms in Table 1 of the text.

An advantage of this method is that we can find easily the relations, among invariants, depending on the space dimension[14][5]. The antisymmetricity with

respect to the "vertical" boxes in the Young tableaus require, to give a nonvanishing invariant after the contraction, that the number of space (and time) coordinates is larger than or equal to the maximum number of rows. For example, the $\{2222\}$ invariant is zero if the space dimension is less than four, so that it gives one identity among the invariants. In $(\partial\partial h)^2$-invariants, we find that if the dimension $n = 1$, the independent invariant is one. If $n = 2$,there are 8, if $n = 3$, 12, if $n \geq 4$, 13.

Appendix B. Adjacency Matrices for $(\partial^3 h)^2$- and $(\partial^4 h \partial^2 h)$- invariants

In this appendix, we list the complete and independent $(\partial\partial\partial h)^2$- and $(\partial\partial\partial\partial h\partial\partial h)$-invariants. The corresponding graphs for them are given in Ref.[5]. We introduce an important new index by two definitions.

Def 9 Let us consider a general SO(n)-invariant of a binary type: $\partial^r h \cdot \partial^s h,\ r + s =$ even. (We explicitly consider the cases of $(r = 3, s = 3)$ and $(r = 4, s = 2)$.) The invariant $\partial^r h \cdot \partial^s h$ is represented by a graph with $(r + s + 4)/2$ suffix-lines where each of them connects two vertices in the graph. We define *bridge-lines* as those suffix-lines which connect a vertex of one bond with another vertex of the other bond.

Def 10 For a general SO(n)-invariant of a binary type: $\partial^r h \cdot \partial^s h,\ r + s =$ even, we define *bridge number* (bridgeno) as the number of bridge-lines of the graph.

bridgeno must be an odd (even) number for $r =$odd (even). The discrimination of invariants can be done mainly by bridgeno and the number of suffix-loops, $\underline{l}$, which is defined in Sec.7 of the text. We give the representatives of the adjacency matrices. These are determined from the conditions (19) and (21) in Sec.4. The index, bridgeno, defined above can be read from a matrix as follows.

$$A = [a_{IJ}];\ I, J = 1, \bar{1}, 2, \bar{2} \quad ,$$
$$\text{bridgeno} = a_{12} + a_{1\bar{2}} + a_{\bar{1}2} + a_{\bar{1}\bar{2}} (= a_{21} + a_{2\bar{1}} + a_{\bar{2}1} + a_{\bar{2}\bar{1}}) \quad . \tag{50}$$

(i) $(\partial^3 h)^2$ invariants

$$4F1 = \partial^2\partial_\mu h_{\lambda\lambda}\partial^2\partial_\mu h_{\rho\rho} \simeq \begin{bmatrix} 2 & 0 & 1 & 0 \\ 0 & 2 & 0 & 0 \\ 1 & 0 & 2 & 0 \\ 0 & 0 & 0 & 2 \end{bmatrix}, 3F1a = \partial^2\partial_\mu h_{\lambda\lambda}\partial^2\partial_\nu h_{\mu\nu} \simeq \begin{bmatrix} 2 & 0 & 0 & 1 \\ 0 & 2 & 0 & 0 \\ 0 & 0 & 2 & 1 \\ 1 & 0 & 1 & 0 \end{bmatrix},$$

$$
\begin{aligned}
3F1b = \partial^2\partial_\mu h_{\nu\nu}\partial_\mu\partial_\lambda\partial_\rho h_{\lambda\rho} \simeq \begin{bmatrix} 2 & 0 & 1 & 0 \\ 0 & 2 & 0 & 0 \\ 1 & 0 & 0 & 2 \\ 0 & 0 & 2 & 0 \end{bmatrix}, 2F1a = \partial^2\partial_\mu h_{\mu\nu}\partial^2\partial_\lambda h_{\lambda\nu} \simeq \begin{bmatrix} 2 & 1 & 0 & 0 \\ 1 & 0 & 0 & 1 \\ 0 & 0 & 2 & 1 \\ 0 & 1 & 1 & 0 \end{bmatrix}, \\
3F3b = \partial^2\partial_\mu h_{\lambda\rho}\partial^2\partial_\mu h_{\lambda\rho} \simeq \begin{bmatrix} 2 & 0 & 1 & 0 \\ 0 & 0 & 0 & 2 \\ 1 & 0 & 2 & 0 \\ 0 & 2 & 0 & 0 \end{bmatrix}, 2F3a = \partial^2\partial_\mu h_{\lambda\rho}\partial^2\partial_\lambda h_{\mu\rho} \simeq \begin{bmatrix} 2 & 0 & 0 & 1 \\ 0 & 0 & 1 & 1 \\ 0 & 1 & 2 & 0 \\ 1 & 1 & 0 & 0 \end{bmatrix}, \\
3F3c = \partial^2\partial_\mu h_{\nu\lambda}\partial_\mu\partial_\nu\partial_\lambda h_{\rho\rho} \simeq \begin{bmatrix} 2 & 0 & 1 & 0 \\ 0 & 0 & 2 & 0 \\ 1 & 2 & 0 & 0 \\ 0 & 0 & 0 & 2 \end{bmatrix}, 3F3a = \partial_\mu\partial_\nu\partial_\lambda h_{\rho\rho}\partial_\mu\partial_\nu\partial_\lambda h_{\sigma\sigma} \simeq \begin{bmatrix} 0 & 0 & 3 & 0 \\ 0 & 2 & 0 & 0 \\ 3 & 0 & 0 & 0 \\ 0 & 0 & 0 & 2 \end{bmatrix}, \\
2F1c = \partial^2\partial_\mu h_{\mu\nu}\partial_\nu\partial_\lambda\partial_\rho h_{\lambda\rho} \simeq \begin{bmatrix} 2 & 1 & 0 & 0 \\ 1 & 0 & 1 & 0 \\ 0 & 1 & 0 & 2 \\ 0 & 0 & 2 & 0 \end{bmatrix}, 2F3b = \partial^2\partial_\mu h_{\nu\lambda}\partial_\nu\partial_\lambda\partial_\rho h_{\mu\rho} \simeq \begin{bmatrix} 2 & 0 & 0 & 1 \\ 0 & 0 & 2 & 0 \\ 0 & 2 & 0 & 1 \\ 1 & 0 & 1 & 0 \end{bmatrix}, \\
2F3c = \partial^2\partial_\mu h_{\nu\lambda}\partial_\mu\partial_\nu\partial_\rho h_{\lambda\rho} \simeq \begin{bmatrix} 2 & 0 & 1 & 0 \\ 0 & 0 & 1 & 1 \\ 1 & 1 & 0 & 1 \\ 0 & 1 & 1 & 0 \end{bmatrix}, 3F3d = \partial_\lambda\partial_\rho\partial_\nu h_{\mu\mu}\partial_\lambda\partial_\rho\partial_\sigma h_{\nu\sigma} \simeq \begin{bmatrix} 0 & 0 & 2 & 1 \\ 0 & 2 & 0 & 0 \\ 2 & 0 & 0 & 1 \\ 1 & 0 & 1 & 0 \end{bmatrix}, \\
2F1b = \partial_\mu\partial_\nu\partial_\sigma h_{\mu\nu}\partial_\lambda\partial_\rho\partial_\sigma h_{\lambda\rho} \simeq \begin{bmatrix} 0 & 2 & 1 & 0 \\ 2 & 0 & 0 & 0 \\ 1 & 0 & 0 & 2 \\ 0 & 0 & 2 & 0 \end{bmatrix}, 2F3d = \partial_\mu\partial_\nu\partial_\lambda h_{\mu\rho}\partial_\nu\partial_\lambda\partial_\sigma h_{\rho\sigma} \simeq \begin{bmatrix} 0 & 1 & 2 & 0 \\ 1 & 0 & 0 & 1 \\ 2 & 0 & 0 & 1 \\ 0 & 1 & 1 & 0 \end{bmatrix}, \\
2F3e = \partial_\mu\partial_\nu\partial_\lambda h_{\mu\rho}\partial_\nu\partial_\rho\partial_\sigma h_{\lambda\sigma} \simeq \begin{bmatrix} 0 & 1 & 1 & 1 \\ 1 & 0 & 1 & 0 \\ 1 & 1 & 0 & 1 \\ 1 & 0 & 1 & 0 \end{bmatrix}, 3F5 = \partial_\mu\partial_\nu\partial_\lambda h_{\rho\sigma}\partial_\mu\partial_\nu\partial_\lambda h_{\rho\sigma} \simeq \begin{bmatrix} 0 & 0 & 3 & 0 \\ 0 & 0 & 0 & 2 \\ 3 & 0 & 0 & 0 \\ 0 & 2 & 0 & 0 \end{bmatrix}, \\
2F5b = \partial_\mu\partial_\nu\partial_\lambda h_{\rho\sigma}\partial_\mu\partial_\nu\partial_\rho h_{\lambda\sigma} \simeq \begin{bmatrix} 0 & 0 & 2 & 1 \\ 0 & 0 & 1 & 1 \\ 2 & 1 & 0 & 0 \\ 1 & 1 & 0 & 0 \end{bmatrix}, 2F5a = \partial_\mu\partial_\nu\partial_\lambda h_{\rho\sigma}\partial_\mu\partial_\rho\partial_\sigma h_{\nu\lambda} \simeq \begin{bmatrix} 0 & 0 & 1 & 2 \\ 0 & 0 & 2 & 0 \\ 1 & 2 & 0 & 0 \\ 2 & 2 & 0 & 0 \end{bmatrix},
\end{aligned}
\tag{51}
$$

The naming of invariants follows the rule: the first number shows that of the suffix-loops ($\underline{l}$), the last number shows that of the bridge number ($\underline{bridgeno}$). It is the same for the next case (ii). The lowest order of $\nabla R \times \nabla R$-invariants are given by the linear combination of the above listed terms.

$$
\begin{aligned}
O_1 = \nabla^\mu R \cdot \nabla_\mu R &= (2F1b) - 2(3F1b) + (4F1) \quad , \\
O_2 = \nabla^\mu R_{\lambda\sigma} \cdot \nabla_\mu R^{\lambda\sigma} &= -(2F3c) - (3F3d) + \frac{1}{2}\{(2F3d) + (2F3e) + (3F3c)\} \\
&\quad + \frac{1}{4}\{(3F3a) + (3F3b)\} \quad , \\
O_3 = \nabla^\mu R^{\lambda\rho\sigma\tau} \cdot \nabla_\mu R_{\lambda\rho\sigma\tau} &= (2F5a) - 2(2F5b) + (3F5) \quad , \\
O_4 = \nabla^\mu R_{\lambda\nu} \cdot \nabla^\nu R^\lambda{}_\mu &= -(3F3d) + \frac{1}{2}\{-(2F3b) - (2F3c) + (3F3c)\}
\end{aligned}
$$

$$+\frac{1}{4}\{(2F3a)+3(2F3d)+(2F3e)+(3F3a)\} \quad , \quad (52)$$

(ii) $(\partial^4 h \partial^2 h)$-invariants

$$P'P=\partial^2\partial^2 h_{\lambda\lambda}\partial^2 h_{\rho\rho}\simeq\begin{bmatrix}4&0&0&0\\0&2&0&0\\0&0&2&0\\0&0&0&2\end{bmatrix}, P'Q=\partial^2\partial^2 h_{\lambda\lambda}\partial_\mu\partial_\nu h_{\mu\nu}\simeq\begin{bmatrix}4&0&0&0\\0&2&0&0\\0&0&0&2\\0&0&2&0\end{bmatrix},$$

$$4H2b=\partial^2\partial^2 h_{\lambda\rho}\partial^2 h_{\lambda\rho}\simeq\begin{bmatrix}4&0&0&0\\0&0&0&2\\0&0&2&0\\0&2&0&0\end{bmatrix}, 4H2a=\partial^2\partial^2 h_{\mu\nu}\partial_\mu\partial_\nu h_{\lambda\lambda}\simeq\begin{bmatrix}4&0&0&0\\0&0&2&0\\0&2&0&0\\0&0&0&2\end{bmatrix},$$

$$3H2a=\partial^2\partial^2 h_{\mu\nu}\partial_\mu\partial_\lambda h_{\nu\lambda}\simeq\begin{bmatrix}4&0&0&0\\0&0&1&1\\0&1&0&1\\0&1&1&0\end{bmatrix}, Q'P=\partial^2\partial_\mu\partial_\nu h_{\mu\nu}\partial^2 h_{\lambda\lambda}\simeq\begin{bmatrix}2&0&0&0\\0&2&0&0\\0&0&2&2\\0&0&2&0\end{bmatrix},$$

$$4H2d=\partial^2\partial_\mu\partial_\nu h_{\lambda\lambda}\partial^2 h_{\mu\nu}\simeq\begin{bmatrix}2&0&0&2\\0&2&0&0\\0&0&2&0\\2&0&0&0\end{bmatrix}, 4H2c=\partial^2\partial_\mu\partial_\nu h_{\lambda\lambda}\partial_\mu\partial_\nu h_{\rho\rho}\simeq\begin{bmatrix}2&0&2&0\\0&2&0&0\\2&0&0&0\\0&0&0&2\end{bmatrix},$$

$$3H2b=\partial^2\partial_\mu\partial_\nu h_{\lambda\lambda}\partial_\mu\partial_\rho h_{\nu\rho}\simeq\begin{bmatrix}2&0&1&1\\0&2&0&0\\1&0&0&1\\1&0&1&0\end{bmatrix}, 3H2d=\partial^2\partial_\mu\partial_\nu h_{\mu\lambda}\partial^2 h_{\nu\lambda}\simeq\begin{bmatrix}2&1&0&1\\1&0&0&1\\0&0&2&0\\1&1&0&0\end{bmatrix},$$

$$3H2c=\partial^2\partial_\mu\partial_\nu h_{\mu\lambda}\partial_\nu\partial_\lambda h_{\rho\rho}\simeq\begin{bmatrix}2&1&1&0\\1&0&1&0\\1&1&0&0\\0&0&0&2\end{bmatrix}, Q'Q=\partial^2\partial_\mu\partial_\nu h_{\mu\nu}\partial_\lambda\partial_\rho h_{\lambda\rho}\simeq\begin{bmatrix}2&2&0&0\\2&0&0&0\\0&0&0&2\\0&0&2&0\end{bmatrix},$$

$$2H2b=\partial^2\partial_\mu\partial_\nu h_{\mu\lambda}\partial_\nu\partial_\rho h_{\lambda\rho}\simeq\begin{bmatrix}2&1&1&0\\1&0&0&1\\1&0&0&1\\0&1&1&0\end{bmatrix}, 2H2a=\partial^2\partial_\mu\partial_\nu h_{\mu\lambda}\partial_\lambda\partial_\rho h_{\nu\rho}\simeq\begin{bmatrix}2&1&0&1\\1&0&1&0\\0&1&0&1\\1&0&1&0\end{bmatrix},$$

$$3H4b=\partial^2\partial_\mu\partial_\nu h_{\lambda\rho}\partial_\mu\partial_\nu h_{\lambda\rho}\simeq\begin{bmatrix}2&0&2&0\\0&0&0&2\\2&0&0&0\\0&2&0&0\end{bmatrix}, 3H4c=\partial^2\partial_\mu\partial_\nu h_{\lambda\rho}\partial_\lambda\partial_\rho h_{\mu\nu}\simeq\begin{bmatrix}2&0&0&2\\0&0&2&0\\0&2&0&0\\2&0&0&0\end{bmatrix},$$

$$2H4c=\partial^2\partial_\mu\partial_\nu h_{\lambda\rho}\partial_\mu\partial_\lambda h_{\nu\rho}\simeq\begin{bmatrix}2&0&1&1\\0&0&1&1\\1&1&0&0\\1&1&0&0\end{bmatrix}, 3H2f=\partial_\mu\partial_\nu\partial_\lambda\partial_\rho h_{\lambda\rho}\partial^2 h_{\mu\nu}\simeq\begin{bmatrix}2&0&0&0\\0&0&2&0\\0&2&0&2\\0&0&2&0\end{bmatrix},$$

$$3H2e=\partial_\mu\partial_\nu\partial_\rho\partial_\sigma h_{\rho\sigma}\partial_\mu\partial_\nu h_{\lambda\lambda}\simeq\begin{bmatrix}0&0&2&0\\0&2&0&0\\2&0&0&2\\0&0&2&0\end{bmatrix}, 3H4a=\partial_\mu\partial_\nu\partial_\lambda\partial_\rho h_{\sigma\sigma}\partial_\mu\partial_\nu h_{\lambda\rho}\simeq\begin{bmatrix}0&0&2&2\\0&2&0&0\\2&0&0&0\\2&0&0&0\end{bmatrix},$$

$$2H2c = \partial_\mu\partial_\nu\partial_\lambda\partial_\rho h_{\mu\nu}\partial_\lambda\partial_\sigma h_{\rho\sigma} \simeq \begin{bmatrix} 0 & 2 & 1 & 1 \\ 2 & 0 & 0 & 0 \\ 1 & 0 & 0 & 1 \\ 1 & 0 & 1 & 0 \end{bmatrix}, 2H4a = \partial_\mu\partial_\nu\partial_\lambda\partial_\rho h_{\mu\sigma}\partial_\nu\partial_\lambda h_{\rho\sigma} \simeq \begin{bmatrix} 0 & 1 & 2 & 1 \\ 1 & 0 & 0 & 1 \\ 2 & 0 & 0 & 0 \\ 1 & 1 & 0 & 0 \end{bmatrix},$$

$$2H4b = \partial_\mu\partial_\nu\partial_\lambda\partial_\rho h_{\mu\sigma}\partial_\nu\partial_\sigma h_{\lambda\rho} \simeq \begin{bmatrix} 0 & 1 & 1 & 2 \\ 1 & 0 & 1 & 0 \\ 1 & 1 & 0 & 0 \\ 2 & 0 & 0 & 0 \end{bmatrix}, \quad (53)$$

The lowest order of $\nabla\nabla R \times R$-invariants are given by the linear combination of the above listed terms.

$$\begin{aligned} T_1 &= \nabla^2 R \cdot R = (Q'Q) - (Q'P) - (P'Q) + (P'P) \quad , \\ T_2 = \nabla^2 R_{\lambda\sigma} \cdot R^{\lambda\sigma} &= \frac{1}{2}\{(2H2a) + (2H2b) - (3H2a) - (3H2b) - (3H2c) - (3H2d)\} \\ &\quad + \frac{1}{4}\{(4H2a) + (4H2b) + (4H2c) + (4H2d)\} \quad , \\ T_3 &= \nabla^2 R_{\lambda\rho\sigma\tau} \cdot R^{\lambda\rho\sigma\tau} = -2(2H4c) + (3H4b) + (3H4c) \quad , \\ T_4 &= \nabla^\mu\nabla^\nu R \cdot R_{\mu\nu} = (2H2c) - (3H2b) \\ &\quad + \frac{1}{2}\{-(3H2e) - (3H2f) + (4H2c) + (4H2d)\} \quad . \quad (54) \end{aligned}$$

Appendix C. Calculation of $\underline{\text{bcn}}[\ ]$ and $\underline{\text{vcn}}[\ ]$

We explain how to calculate the indices, $\underline{\text{bcn}}[\ ]$ and $\underline{\text{vcn}}[\ ]$ in the actual(computer) calculation. Let us consider a $(\partial\partial h)^2$-invariant. It has two bonds. As an example, we take C1 in Fig.24.

Def 11 We assign i=0 for one bond and i=1 for the other. 'i' is the *bond number* and discriminates the two bonds. Next we assign j=0 for all dd-vertices and j=1 for all h-vertices. 'j' is the *vertex-type number* and discriminate the vertex-type. Any vertex in a graph is specified by a pair (i,j).

Def 12 When we trace a suffix-line, along a loop, starting from a vertex (i_0,j_0) in a certain direction, we pass some vertices, $(i_1,j_1),(i_2,j_2),\cdots$ and finally come back to the starting vertex (i_0,j_0). We focus on the *change* of the bond number, i, and the vertex-type number, j, when we pass from a vertex to the next vertex in the tracing (see Fig.25 and 18). For k-th loop, we assign as $\sum_{\text{along } k\text{-th loop}} |\Delta i| \equiv \underline{\text{bcn}}[k]$, $\sum_{\text{along } k\text{-th loop}} |\Delta j| \equiv \underline{\text{vcn}}[k]$.

$\underline{\text{bcn}}[\ ]$ and $\underline{\text{vcn}}[\ ]$ are listed for all $(\partial\partial h)^2$-invariants in Table 1. $\underline{\text{bcn}}[\ ]$ and $\underline{\text{vcn}}[\ ]$ defined above satisfy the following important properties.

1. They donot depend on the starting vertex for tracing along a loop.
2. They donot depend on the direction of the tracing.

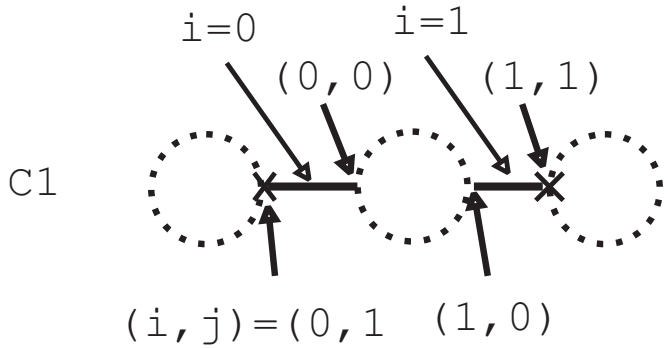

Fig.24 Bond number 'i' and vertex-type number 'j' for each vertex in the invariant C1.

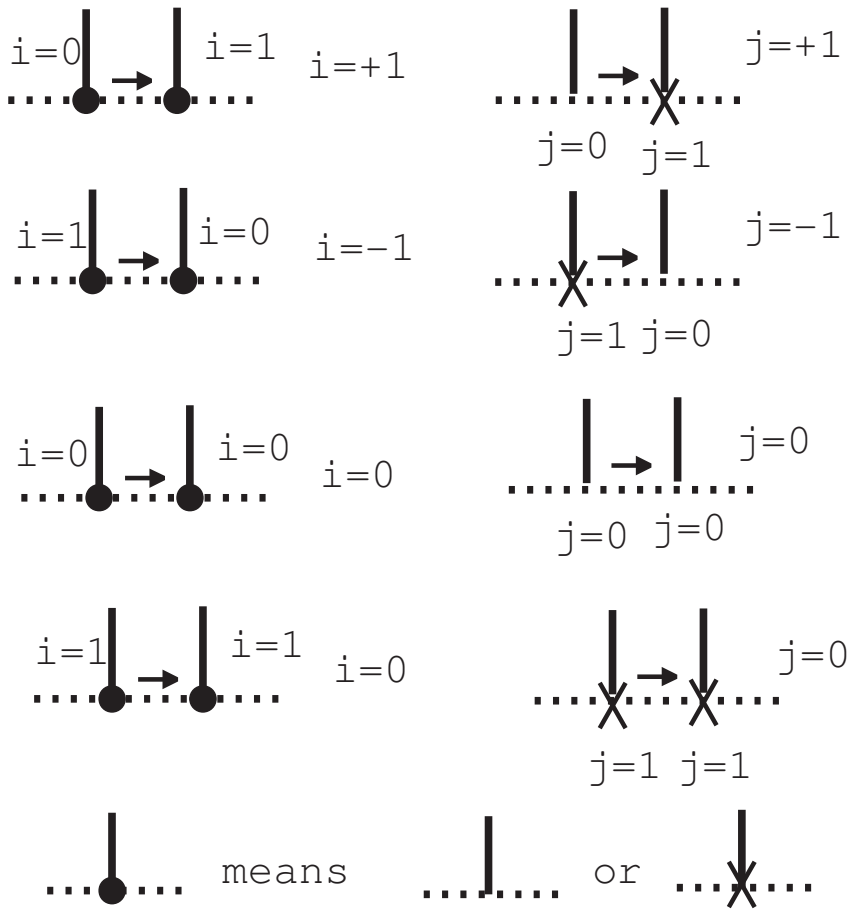

Fig. 25 Change of i (bond number) and j (vertex-type number). Arrows indicate directions of tracings.

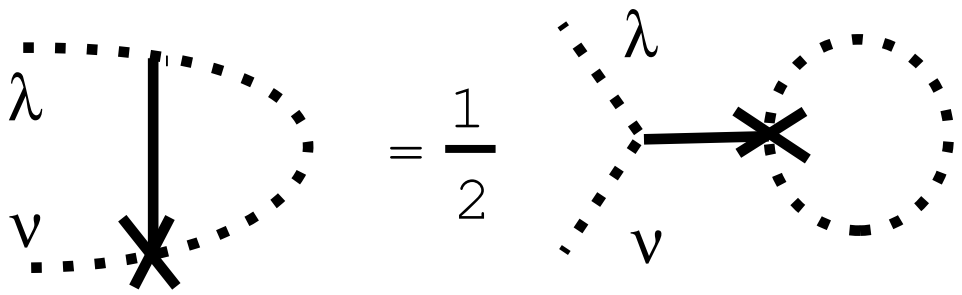

Fig.26 Graphical rule, expressing (56), due to the gauge-fixing condition (55) .

Appendix D. Gauge-Fixing Condition and Graphical Rule

In the text, we have not taken a gauge-fixing condition. When we calculate a physical quantity in the classical and quantum gravity, we sometimes need to impose the condition on the metric $g_{\mu\nu}$ for some reasons. Firstly, in the case of quantizing gravity itself or of solving a classical field equation with respect to the gravity mode, we *must* impose the fixing condition in order to eliminate the local freedom ($\epsilon^{\mu}(x), \mu = 1, 2, \cdots, n-1, n.$) due to the general coordinate invariance (2): $g_{\mu\nu} \to g_{\mu\nu} + g_{\mu\lambda}\nabla_{\nu}\epsilon^{\lambda} + g_{\nu\lambda}\nabla_{\mu}\epsilon^{\lambda}$. Secondly, even when the condition is theoretically not necessary (such as the quantization on the fixed curved space, or the ordinary anomaly calculation), the gauge-fixing is practically useful because it considerably reduces the number of SO(n) invariants to be considered.

In the weak gravity case $g_{\mu\nu} = \delta_{\mu\nu} + h_{\mu\nu}$, $|h_{\mu\nu}| \ll 1$, the condition is expressed by $h_{\mu\nu}$. Let us take a familiar gauge:

$$\partial_{\mu}h_{\mu\nu} = \frac{1}{2}\partial_{\nu}h \quad , \quad h \equiv h_{\lambda\lambda} \quad . \tag{55}$$

This condition leads to the following condition on the present basic element $\partial_{\mu}\partial_{\nu}h_{\alpha\beta}$.

$$\partial_{\lambda}\partial_{\mu}h_{\mu\nu} = \frac{1}{2}\partial_{\lambda}\partial_{\nu}h \quad , \quad h \equiv h_{\lambda\lambda} \quad . \tag{56}$$

This gives us a graphical rule shown in Fig.26.

Let us see how does this rule reduce the number of independent invariants given in the text. For $\partial\partial h$-invariants, we obtain the following relation

$$Q = \frac{1}{2}P \quad . \tag{57}$$

For $(\partial\partial h)^2$-invariants, we obtain the following relations.

$$A2 = A3 = \frac{1}{2}B1 = \frac{1}{4}C1 \quad ,$$
$$B2 = \frac{1}{2}C3 \quad , \quad QQ = \frac{1}{2}PQ = \frac{1}{4}PP \quad . \tag{58}$$

Therefore, in the gauge (55), we can reduce the number of independent invariants from 2 to 1 for $\partial\partial h$-invariants (,say, P) and from 13 to 7 for $(\partial\partial h)^2$-invariants (,say, $A1, B3, B4, C1, C2, C3, PP$).

We expect this gauge-fixed treatment is practically very useful when the quantity under consideration is known to be gauge-invariant in advance.

References

[1] E. Alvarez, *Rev.Mod.Phys.***61** (1989) 561.

[2] H. Weyl, The Classical Group, their Invariants and Representations (Princeton), 1938.

[3] D.E. Littlewood, The Theory of Group Characters and Matrix Representations of Groups 2nd edn (Oxford: Clarendon), 1950.

[4] S.A. Fulling, R.C. King, B.G. Wybourne and C.J. Cummins, *Class.Quantum Grav.***9** (1992) 1151.

[5] S. Ichinose and N. Ikeda, *Jour.Math.Phys.***38** (1997) 6475.

[6] F. Harary, Graph Theory (Reading-Menlo Park-Ontario: Addison-Wesley Pub.Co.), 1969.

[7] S. Ichinose and N. Ikeda, Univ. of Shizuoka preprint, US-98-07, BNL-preprint, hep-th/9810256, "Weyl Anomaly in Higher Dimensions and Feynman Rules in Coordinate Space".

[8] N. Nakanishi, Graph Theory and Feynman Integral (New York-London-Paris: Gordon and Breach,Science Publisher), 1971.

[9] S. Ichinose, hep-th/9609014, *Int.Jour.Mod.Phys.***C9**(1998)243.

[10] N.D. Birrel and P.C. Davies, Quantum Fields in Curved Space (Cambridge: Cambridge Univ. Press), 1982.

[11] S. Ichinose and N. Ikeda, *Phys.Rev.***D53** (1996) 5932.

[12] G. t'Hooft and M. Veltman, *Ann.Inst.H.Poincaré* **20** (1974) 69.

[13] S. Ichinose and M. Omote, *Nucl.Phys.***B203** (1982) 221.

[14] S. Ichinose, *Class.Quantum Grav.***12** (1995) 1021.

Figure Captions

- Fig.1 (a) (k+2)-tensor (9); (b) 4-tensor $\partial_\mu\partial_\nu h_{\alpha\beta}$
- Fig.2 2-tensors of $\partial^2 h_{\alpha\beta}$, $\partial_\mu\partial_\nu h_{\alpha\alpha}$ and $\partial_\mu\partial_\beta h_{\alpha\beta}$
- Fig.3 Invariants of $P \equiv \partial_\mu\partial_\mu h_{\alpha\alpha}$ and $Q \equiv \partial_\alpha\partial_\beta h_{\alpha\beta}$.
- Fig.4 Feynman rule of the Lagrangian (11).
- Fig.5 Graph of (7).
- Fig.6 Two vertices are connected by k dotted lines. •-vertex represents a der-vertex or a h-vertex.
- Fig.7 A vertex is connected with itself by l dotted lines. •-vertex represents a der-vertex or a h-vertex.
- Fig.8 Graphical Representations of $\partial_\mu\partial_\nu h_{\alpha\beta}\partial_\mu\partial_\nu h_{\gamma\delta}$ and $\partial_\mu\partial_\nu h_{\alpha\beta}\partial_\nu\partial_\lambda h_{\lambda\beta}$.
- Fig.9 Two ways to place two dd-vertices (small circles) and two h-vertices (cross marks) upon one suffix-loop.
- Fig.10 Three independent $(\partial\partial h)^2$-invariants for the case of one suffix-loop.
- Fig.11 Bondless diagrams for (26).
- Fig.12 Five independent $(\partial\partial h)^2$-invariants for the case of two suffix-loops.
- Fig.13 Three bondless diagrams corresponding to (27).
- Fig.14 Four independent $(\partial\partial h)^2$-invariants for the case of three suffix-loops.
- Fig.15 The bondless diagram corresponding to (28).
- Fig.16 The unique independent $(\partial\partial h)^2$-invariant for the case of four suffix-loops.
- Fig.17 Graph B1 for the weight calculation (31).
- Fig.18 Explanation of $\underline{\text{bcn}}[\ ]$ and $\underline{\text{vcn}}[\ ]$ using Graph A2.
- Fig.19 Graph G9$\equiv \partial_\mu\partial_\omega h_{\mu\nu}\cdot\partial_\nu\partial_\lambda h_{\tau\sigma}\cdot\partial_\lambda\partial_\sigma h_{\tau\omega}$.
- Fig.20 Graph of G25$\equiv \partial_\mu\partial_\nu h_{\lambda\sigma}\cdot\partial_\sigma\partial_\tau h_{\mu\nu}\cdot\partial_\lambda\partial_\omega h_{\tau\omega}$.
- Fig.21 Graphical representation of weak expansion of Riemann tensors .
- Fig.22 Lowest order graphs for the Weyl anomaly calculation (44):
  [2 dim] (a1) $\partial^2 h \simeq \begin{bmatrix}2&0\\0&2\end{bmatrix}$, (a2) $\partial_\mu\partial_\nu h_{\mu\nu} \simeq \begin{bmatrix}0&2\\2&0\end{bmatrix}$;
  [4 dim] (b1) $(\partial^2)^2 h \simeq \begin{bmatrix}4&0\\0&2\end{bmatrix}$, (b2) $\partial^2\partial_\mu\partial_\nu h_{\mu\nu} \simeq \begin{bmatrix}2&2\\2&0\end{bmatrix}$;

[6 dim] (c1) $(\partial^2)^3 h \simeq \begin{bmatrix} 6 & 0 \\ 0 & 2 \end{bmatrix}$, (c2) $(\partial^2)^2 \partial_\mu \partial_\nu h_{\mu\nu} \simeq \begin{bmatrix} 4 & 2 \\ 2 & 0 \end{bmatrix}$;
[8 dim] (d1) $(\partial^2)^4 h \simeq \begin{bmatrix} 8 & 0 \\ 0 & 2 \end{bmatrix}$, (d2) $(\partial^2)^3 \partial_\mu \partial_\nu h_{\mu\nu} \simeq \begin{bmatrix} 6 & 2 \\ 2 & 0 \end{bmatrix}$;
[10 dim] (e1) $(\partial^2)^5 h \simeq \begin{bmatrix} 10 & 0 \\ 0 & 2 \end{bmatrix}$, (e2) $(\partial^2)^4 \partial_\mu \partial_\nu h_{\mu\nu} \simeq \begin{bmatrix} 8 & 2 \\ 2 & 0 \end{bmatrix}$.

- Fig.23 (a) $\partial_\alpha \partial_\kappa h_{\alpha\beta} \cdot \partial_\beta \partial_\mu h_{\mu\nu} \cdot \partial_\nu \partial_\lambda h_{\lambda\sigma} \cdot \partial_\sigma \partial_\tau h_{\tau\omega} \cdot \partial_\omega \partial_\theta h_{\theta\kappa}$ and (b) $\partial_\tau \partial_\omega h_{\mu\nu} \cdot \partial_\mu \partial_\beta h_{\omega\theta} \cdot \partial_\alpha \partial_\beta h_{\nu\lambda} \cdot \partial_\lambda \partial_\sigma h_{\alpha\kappa} \cdot \partial_\kappa \partial_\theta h_{\sigma\tau}$.

- Fig.24 Bond number 'i' and vertex-type number 'j' for each vertex in the invariant C1.

- Fig. 25 Change of i (bond number) and j (vertex-type number). Arrows indicate directions of tracings.

- Fig.26 Graphical rule, expressing (56), due to the gauge-fixing condition (55) .